TAMPEREEN TEKNILLINEN YLIOPISTO
TAMPERE UNIVERSITY OF TECHNOLOGY

Jaakko Yli-Ojanperä

Calibration of Aerosol Instruments in a Wide Particle Size Range

Julkaisu 1079 • Publication 1079

Tampere 2012

Tampereen teknillinen yliopisto. Julkaisu 1079
Tampere University of Technology. Publication 1079

Jaakko Yli-Ojanperä

Calibration of Aerosol Instruments in a Wide Particle Size Range

Thesis for the degree of Doctor of Science in Technology to be presented with due permission for public examination and criticism in Sähkötalo Building, Auditorium S2, at Tampere University of Technology, on the 2nd of November 2012, at 12 noon.

Tampereen teknillinen yliopisto - Tampere University of Technology
Tampere 2012

Doctoral candidate: Jaakko Yli-Ojanperä, M.Sc
Aerosol Physics Laboratory
Department of Physics
Tampere University of Technology

Supervisors: Jorma Keskinen, prof.
Aerosol Physics Laboratory
Department of Physics
Tampere University of Technology

Jyrki Mäkelä, prof.
Aerosol Physics Laboratory
Department of Physics
Tampere University of Technology

Pre-examiners: Tuukka Petäjä, PhD
Division of Atmospheric Sciences
Department of Physics
University of Helsinki

Wladyslaw W. Szymanski, prof.
Aerosol Physics and Environmental Physics
Faculty of Physics
University of Vienna

Opponent: Susanne V. Hering, PhD
Aerosol Dynamics Inc.
Berkeley
United States

ISBN 978-952-15-2925-2 (printed)
ISBN 978-952-15-3023-4 (PDF)
ISSN 1459-2045

Abstract

Aerosol particles have an important role in many scientific and technological issues. Aerosol particle measurements are widely applied for example in clean room technology, in atmospheric measurements and in studying the Particulate Matter (PM) emissions from traffic and industry. This thesis concentrates on developing new aerosol instrumentation both for measurement and calibration purposes. On the measurement side, the driving force has been the urgent need for instruments that have a fast time response and are able to measure nanoparticles with reasonable accuracy. In this respect, the nanoparticle resolution of the Electrical Low Pressure Impactor (ELPI, Dekati Ltd.) was improved by designing, manufacturing and implementing a new impactor stage (cutpoint 16.7 nm) to the ELPI cascade impactor. The new impactor stage divides the particle size range measured by the filter stage (7–30 nm) between the new stage and the filter stage. As a result, the nanoparticle resolution of the ELPI was improved. This made the device more suitable, for example, for vehicle engine emission measurements. The new stage is currently being sold as a part of the new ELPI+ instrument, which is an improved version of the original ELPI.

On the calibration side, the main driving force behind aerosol instrument development has been the lack of calibration standards available for calibrating the number concentration responses of the instruments in the sub-micrometer size range. In this size range, the most common method to calibrate an instrument is to use a differential mobility analyzer (DMA), for obtaining monodisperse particles for the calibration, and a Faraday cup aerosol electrometer (FCAE), for measuring the reference number concentration. Even though, in principle, the DMA allows size selection up to 1 μm in diameter, the calibrations are usually limited to particles below 100 nm because of the multiple charging of particles.

To solve this problem, a new concept for realizing a number concentration standard in a wide size range was introduced. In this concept, a novel principle of first charging nanoparticles and growing them afterwards to much larger particle sizes is applied for the generation of the singly charged, fairly monodisperse calibration aerosols. Combined with an FCAE this concept, ideally, solves the calibration issues in the sub-micrometer size range. In order to test this concept, a new instrument called the Single Charged Aerosol Reference (SCAR) was designed, built and tested. In the first experiments, the SCAR was verified to produce singly charged, fairly monodisperse particle size distributions between 10 and 500 nm in diameter and to be suitable for calibration purposes. As a result of a rigorous validation process, true SI-traceability was obtained for the particle number concentration output of the SCAR, and the calibration of other instruments on the absolute scale became possible. As a final necessary step in becoming an internationally recognized number concentration standard, an intercomparison between the SCAR and two number concentration standards of the National Institute of Advanced Industrial Science and Technology was conducted in Japan. The results obtained with the three standards were found to agree within the uncertainty limits at all overlapping particle sizes. As a consequence, a new primary number concentration standard, which enables accurate calibration of various instruments in the whole sub-micrometer range, was established.

Acknowledgements

This work has been conducted in the Aerosol Physics Laboratory in the Tampere University of Technology (Finland). At first, I would like to express my gratitude to professors Jorma Keskinen and Jyrki Mäkelä for their guidance and support, and for giving me freedom in meeting the objectives of the research projects. I would like to thank the whole Aerosol Physics Group for such an inspiring and pleasant working environment. Mr. Antti Rostedt, Mr. Anssi Arffman and Dr. Marko Marjamäki deserve my deepest thanks for their support and company during and after the working hour. Veli-Pekka Plym and other gentlemen from the mechanical workshop of the Physics Department are truly acknowledged for constructing dozens of valuable prototype instruments for this thesis.

I would like to thank all the co-authors for their important contribution and for the fruitful co-operation. Dr. Martti Heinonen and Mr. Richard Högström from Mikes–Centre for Metrology and Accreditation (Finland) are acknowledged for the co-operation during a joint research project, within which the SCAR has been developed. In particular, I would like to thank Dr. Sakurai Hiromu from the National Institute of Advanced Industrial Science and Technology for giving me an opportunity to visit AIST and to work with you.

This work has been funded by Tekes—the Finnish Funding Agency for Technology and Innovation, Cluster for Energy and Environment (CLEEN Ltd., MMEA, WP 4.5.1), Ministry of Education and the Academy of Finland (project No. 141209) for Graduate School "Atmospheric Composition and Climate Change: From Molecular Processes to Global Observations and Models", Dekati Ltd., Ecocat Oy and Gasmet Technologies Oy which are gratefully acknowledged.

I am grateful to my parents, siblings and to all my friends for being there for me. Finally, I would like to thank my beloved Susanna for her patience, support and understanding throughout my working years at Tampere University of Technology.

List of publications

This thesis is a compound thesis consisting of an introductory review and the following four publications. The publications are cited in the introductory review according to their numbering presented below.

I. Yli-Ojanperä, J., Kannosto, J., Marjamäki, M., Keskinen, J. (2010) Improving the Nanoparticle Resolution of the ELPI. *Aerosol and Air Quality Research* **10**, 360–366.

II. Yli-Ojanperä, J., Mäkelä, J.M., Marjamäki, M., Rostedt, A., Keskinen, J. (2010) Towards traceable particle number concentration standard: Single Charged Aerosol Reference (SCAR). *J. Aerosol Sci.* **41**, 719–728.

III. Högström, R., Yli-Ojanperä, J., Rostedt, A., Iisakka, I., Mäkelä, J.M., Heinonen, M. and Keskinen, J. (2011) Validating the Single Charged Aerosol Reference (SCAR) as a traceable particle number concentration standard for 10 to 500 nm aerosol particles. *Metrologia* **48**, 426–436.

IV. Yli-Ojanperä, J., Sakurai, H., Iida, K., Mäkelä, J.M., Ehara, K. and Keskinen, J. (2012) Comparison of three particle number concentration calibration standards through calibration of a single CPC in a wide particle size range. *Aerosol Sci. Technol.* **46**, 1163–1173.

Author's contribution

I. Yli-Ojanperä, J., Kannosto, J., Marjamäki, M., Keskinen, J. (2010) Improving the Nanoparticle Resolution of the ELPI. *Aerosol and Air Quality Research* **10**, 360–366.

The author had the main responsibility of the paper, except for the section dealing with particle density, and wrote most of the paper.

II. Yli-Ojanperä, J., Mäkelä, J.M., Marjamäki, M., Rostedt, A., Keskinen, J. (2010) Towards traceable particle number concentration standard: Single Charged Aerosol Reference (SCAR). *J. Aerosol Sci.* **41**, 719–728.

The author designed and built the SCAR instrument, conducted all the experiments and wrote most of the paper.

III. Högström, R., Yli-Ojanperä, J., Rostedt, A., Iisakka, I., Mäkelä, J.M., Heinonen, M. and Keskinen, J. (2011) Validating the Single Charged Aerosol Reference (SCAR) as a traceable particle number concentration standard for 10 to 500 nm aerosol particles. *Metrologia* **48**, 426–436.

The first two authors contributed equally to this work. The author had the main responsibility in designing and conducting the validation experiments. The author had the main responsibility in the contents of the paper, except for the uncertainty evaluation of the CPC calibration, and participated in writing.

IV. Yli-Ojanperä, J., Sakurai, H., Iida, K., Mäkelä, J.M., Ehara, K. and Keskinen, J. (2012) Comparison of three particle number concentration calibration standards through calibration of a single CPC in a wide particle size range. *Aerosol Sci. Technol.* **46**, 1163–1173.

The author was responsible for the objectives of the comparison and conducted the experiments with the SCAR. The author decided the contents of the paper and wrote most of the paper.

Contents

Symbols and abbreviations

α_c	Condensation coefficient
β	Concentration bias between sampling ports
γ	Calibration factor of the electrometer
δ	Deviation of the concentration bias from unity
ΔI	Offset corrected current
η	Viscosity of the carrier gas
η_{FCAE}	Detection efficiency of the Faraday cup
ρ_p	Particle density
σ	Surface tension
η_{CPC}	CPC detection efficiency
$s(\bar{x})$	Experimental standard deviation of the component x
m	Mass of a molecule
M	Molecular weight
$s(x)$	Standard deviation of the component x
$u(x)$	Standard uncertainty of the component x
C	Particle number concentration
$C_C(D_p)$	Particle size dependent slip correction factor
D_p	Mobility equivalent particle diameter
e	Elementary charge
I_{offset}	Electrometer offset current
$I_{particle}$	Average current induced by particles
k	Boltzmann constant
n	Number of net elementary charges in a particle
N_A	Avogadro constant
p_∞	Vapor pressure far from the particles
p_s	Saturation vapor pressure over a flat surface
Q	Volumetric flow rate
R	Molar gas constant
T	Temperature
Z	Electrical mobility

AIST	National institute of advanced industrial science and technology
APS	Aerodynamic particle sizer
CAST	Combustion aerosol standard
CPC	Condensation particle counter
DMA	Differential mobility analyzer
DMPS	Differential mobility particle sizer
DOP	Di-octyl phthalate
DOS	Di-octyl sebacate
DUT	Device under test
EAG	Electrospray aerosol generator

EEPS	Engine exhaust particle sizer
ELPI	Electrical low pressure impactor
ESP	Electrostatic precipitator
EUSAAR	European supersites for atmospheric aerosol research
FCAE	Faraday cup aerosol electrometer
FMPS	Fast mobility particle sizer
GMD	Geometric mean diameter
GSD	Geometric standard deviation
HV	High voltage
IAG	Inkjet aerosol generator
LPC	Laser particle counter
MFC	Mass flow controller
NaCl	Sodium chloride
NCS	Number concentration standard
NIST	National institute of standards and technology
NMI	National metrology institute
OPC	Optical particle counter
PAO	Poly-α-olefin
PM	Particulate matter
PSL	Polystyrene latex
SCAR	Single charged aerosol reference
SI	International system of units of measurement
SMPS	Scanning mobility particle sizer
VOAG	Vibrating orifice aerosol generator
WCCAP	World calibration centre for aerosol physics

1. Introduction

Aerosol particles have a major role in many scientific and technology issues, such as the health effects of particulate emissions (CAFE, 2001), and the global climate change (IPCC, 2007) and breakthroughs in nanotechnology (NSF, 2003). Aerosol particle measurements are widely applied, for example, in clean room technology, in atmospheric measurements and in studying the Particulate Matter (PM) emissions from traffic and industry. Often, the studied phenomena are related to properties other than simple mass concentration. As a consequence, properties such as particle size, number concentration, surface area concentration and size distribution are measured, especially in the fine (< 1μm) and ultra-fine (< 100 nm) particle size range. Several instruments, e.g. Optical and Laser Particle Counters (OPC/LPC; e.g. Knollenberg and Luehr, 1976), Condensation Particle Counters (CPC; e.g. Agarwal and Sem, 1980), Aerodynamic Particle Sizers (APS; e.g. Baron, 1984), Scanning Mobility Particle Sizers (SMPS; Wang and Flagan, 1990), Electrical Low Pressure Impactors (ELPI; Keskinen et al., 1992) and a number of fast mobility sizers (FMPS, EEPS, DMS; e.g. Biskos et al., 2005), are capable of measuring these properties.

To some extent, the ongoing development of instruments is guided by the needs of the measurement field and, also, by the current and upcoming legislation. In order to reveal the underlying physics and chemistry in the atmospheric particle formation processes, measurements are required at the very beginning of the particle formation process, during which the particle size can be only about 1.5 nm (Kulmala et al., 2007). In the vehicle PM emission measurements, the composition and the formation of the nucleation mode particles is of particular interest (Kittelson, 1998; Rönkkö et al., 2007). In this application area, the geometric mean diameter of the nucleation mode can be as small as 10 nm (Filippo and Maricq, 2008). Both applications have remarkable requirements for the measurement instruments, as particles down to sizes of the order of 1 nm in terms of an equivalent diameter should be measured with good accuracy and with high time resolution. In this respect, instruments having a fast time response and being able to measure smaller and smaller particles are truly needed.

Together with the development of the instruments, the calibration capabilities must be developed and extended accordingly. In aerosol measurements in general, the particle size can be measured rather accurately because the size response of the instruments can be traceably calibrated against particle size reference materials such as polystyrene latex (PSL) particles. The accuracy of the number concentration measurement is more ambiguous, because no internationally coherent Number Concentration Standard (NCS) exists. Consequently, no easily accessible concentration references, i.e. standards, are available for calibration purposes. This applies especially for particle sizes smaller than 10 nm and for particle sizes between 100 nm and 1 μm. Although number concentration of the particles is not controlled by laws and regulations in the former size range, reliable NCSs in this range would improve the quality of scientific atmospheric studies. The latter range is of particular importance, because number based limits are already applied in this size range in clean rooms of production facilities and for vehicle PM emissions (ISO 14644-1, 1999; European Commission, 2008).

In this thesis, new aerosol instrumentation was developed both for measurement and calibration purposes. On the measurement side, the nanoparticle resolution of the ELPI (Dekati Ltd.) was improved by designing and manufacturing a new impactor stage (cutpoint 16.7 nm) for the ELPI cascade impactor (Paper I). On the calibration side, the main objective was to develop an

accurate primary number concentration standard that would cover the particularly challenging particle size range between 100 nm and 1 μm. The development of a standard requires at least three phases named: *proof of concept, validation,* and *intercomparison*. In the first phase, a new instrument called the Single Charged Aerosol Reference (SCAR) was designed, built and tested (Paper II). This new device combines a novel principle for the generation of a singly charged calibration aerosol (Mirme and Tamm, 2002; Uin et al., 2009) with a traceable Faraday cup Aerosol Electrometer (FCAE) based number concentration measurement in order to realize a number concentration standard. After the SCAR was finalized, it was validated in co-operation with MIKES–the Centre for Metrology and Accreditation (Finland). During this phase, the operation of the SCAR was thoroughly characterized (Paper III). As a result, a true SI-traceability for the particle number concentration output of the SCAR was formed and the calibration of other instruments on the absolute scale became possible. In order to become an internationally recognized number concentration standard, an intercomparison between the SCAR and two number concentration standards of the National Institute of Advanced Industrial Science and Technology (AIST) was conducted in Japan (Paper IV). The consistency of the results is an important step towards establishing internationally coherent particle number concentration standards, which are needed especially for legislative purposes.

This thesis begins with an overview of the existing calibration methods. To this end, special attention is given to the electrical calibration method and to its limitations in the sub-micrometer size range. Next, a new concept and a device (the SCAR) designed to overcome the limitations of the electrical calibration is presented and carefully characterized. In the following section, the overall performance of the SCAR as such and with respect to other standards is evaluated through an example calibration. In the end, the thesis goes back to the very beginning by presenting the most recent status of the existing and upcoming number concentration standards worldwide.

2. Calibration of aerosol instruments

2.1. Motivation

A calibration of an instrument refers to a process, in which the relation between the reading of the instrument and the absolute value of the measured quantity is determined. After the calibration, the instrument can be used for measuring absolute values of the quantity. If the calibration is performed traceably, also the uncertainty of the measurement results can be expressed. A valid and accurate calibration of an instrument is the first step towards conducting accurate measurements. Using the same calibrator for all of the instruments in a measurement network, such as in the project called the European Supersites for Atmospheric Aerosol Research (EUSAAR, webpage; Wiedensohler et al., 2012), ensures comparability of the results. Good opportunities for performing such calibrations for aerosol instruments are the international calibration workshops organized by the World Calibration Centre for Aerosol Physics (WCCAP, webpage). Regular calibrations reveal the changes in the instruments' response, which allows user to conclude whether the changes in the reading over time are real or not. In this sense, accurate measurements are possible only if the changes in the response of the measurement instrument over time are much smaller than the changes in the measured quantity. This is a strict requirement for the applied measurement technique. In some aerosol applications, the performance criteria of the instruments and their calibration come from the recommendations and regulations set by different organizations,

such as the United States Environmental Protection Agency and the International Organization for Standardization. Again, a calibration is needed in order to meet these requirements.

2.2. Overview of existing calibration methods

In aerosol measurements, perhaps the most relevant quantities requiring calibration are the size response and the number concentration response of an instrument, the latter being in the focus of this thesis. The calibration of a continuous flow type instrument usually reduces to the accurate calibration of the inlet flow rate and to the detection efficiency (e.g. CPCs) or the collection efficiency (e.g. impactors) of the instrument. The detection efficiency refers to the instrument's response to a known number concentration, and the collection efficiency refers to the fraction of the particles collected by the instrument from the total amount of particles entering the instrument. The flow rate can be easily calibrated against traceable standards of the international and national metrology institutions, such as NIST in US (Wright et al., 1998) and Mikes in Finland (Sillanpää et al., 2006). However, the calibration of the number concentration response is a much more difficult task as it requires monodisperse particles with a known size and concentration. For many instruments, the operating size and concentration ranges extend over several orders of magnitude, i.e. more than any single calibrator could ever cover. Therefore, calibration methods having different operation principles are needed.

According to Ehara and Sakurai (2010), three conceivable types of NCSs (i.e. calibrators) can be identified for airborne particles: the generator, the reference material and the measurement instrument. In the generator approach, the particle number concentration can be derived directly from the operation parameters. Examples of this type of a standard are the Combustion Aerosol Standard (CAST; Barthazy et al., 2007), and the Inkjet Aerosol Generator (IAG; Iida et al., 2010). The CAST can be used as a particle generator in applications that require soot particles with composition that corresponds very well with particulate emissions from modern diesel operated vehicles (Jing webpage; Schneider et al., 2005; Marshall, 2007), but not as a calibrator by itself. The IAG is more than suitable for verifying the operation of CPCs and OPCs in the field due to the portable nature of the instrument. However, the generator approach cannot be made traceable to SI-units (e.g., kg, A) by itself, which makes it a secondary standard by nature. In the reference material approach, a constant and known number concentration is conserved in a vessel. As a recent attempt, Koch et al. (2008) introduced a method in which an aerosol with a well-defined starting time coagulates in a chamber within which the number concentration can be unambiguously derived from the life time of the aerosol. As a disadvantage, the particle size and number concentration are changing over time, which is unacceptable in calibration measurements.

At the moment, the most widely applied type of an NCS is the measurement instrument approach. In this approach, an instrument with well characterized detection efficiency is used as a number concentration reference. Depending on the particle size, different references can be used. At large particle sizes (diameter > 1μm), the response can be calibrated against a traceable reference measurement of the mass concentration. This method involves the collection of particles with a reference instrument (e.g. a filter holder equipped with a high efficiency filter) operated at a known inlet flow rate. With traceable flow rate and particle mass measurements, the mass concentration is also traceable. Provided that the particles are monodisperse, and the size and the density of the particles are known, also the number concentration can be defined accurately. As an example, Armendariz and Leith (2002) calibrated an Aerodynamic Particle Sizer (APS) against the mass

concentration measured with a cascade impactor. As another example, Volckens and Peters (2005) used a fluorometer to quantify the reference mass concentration from the monodisperse particles generated with a Vibrating Orifice Aerosol Generator (VOAG; Berglund and Liu, 1973). However, the mass based reference method becomes impractical in the fine particle region (diameter < 1 μm) due to prolonged measurement times. As a consequence, other more sensitive references, such as the electrical calibration method that combines a Differential Mobility Analyzer (DMA; Liu et al., 1975) and a Faraday Cup Aerosol Electrometer (FCAE), are used. An FCAE is also used in the NCS developed in this thesis.

3. Electrical calibration method

3.1. Method and applications

In the fine particle region (diameter < 1 μm), a commonly applied number concentration reference is the combination of a Differential Mobility Analyzer and a Faraday Cup Aerosol Electrometer (FCAE). A simplified calibration setup for this approach is shown in Fig. 1.

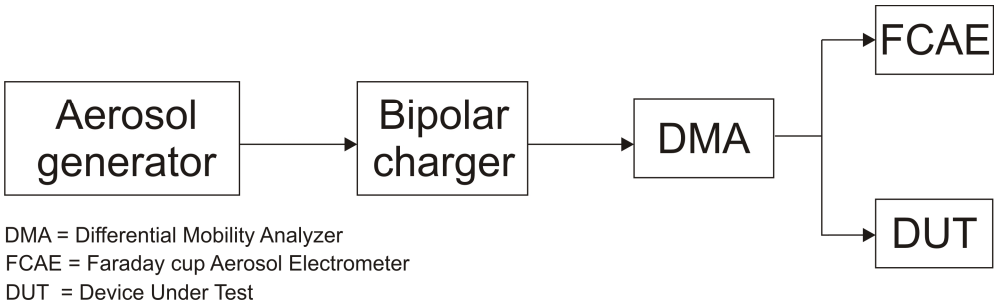

Figure 1. Schematic view of a simplified calibration setup using the electrical calibration method.

In this method, a polydisperse aerosol distribution is first generated and charged bipolarly. A DMA is used for obtaining monodisperse, singly charged particles from the polydisperse distribution for the calibration. The resulting calibration aerosol is divided between the instrument under calibration (DUT in Fig. 1) and the FCAE, which measures the reference number concentration. For a CPC, the detection efficiency is calculated as a ratio of the concentration measured by the CPC to that measured by the FCAE. This calibration method is often used in measuring the counting efficiency curves of various CPCs (e.g. Liu and Kim, 1977; Banse et al., 2001; Sem, 2002; Hermann et al., 2007; Mordas et al., 2008), and it is used as a primary NCS in some of the National Metrology Institutes (NMIs) (Fletcher et al., 2009; Schlatter, 2009; Sakurai and Ehara, 2011).

The operation of the FCAE is based on the electrical detection of particles. It consists of a Faraday cup, a highly sensitive electrometer and accurate instrumentation for the inlet flow measurement and control. A cross-section of the home-built Faraday cup developed for the SCAR in this thesis (Papers II–IV) is shown in Fig. 2. A Faraday cup is a flow through instrument which collects all the particles from the carrier gas onto a high efficiency filter as in Fig. 2. The filter is surrounded by a Faraday cage which is electrically insulated from the grounded outer shield of the cup. By grounding the Faraday cage through an electrometer, a direct measurement of the electric charge carried by the particles can be obtained in the form of electric current.

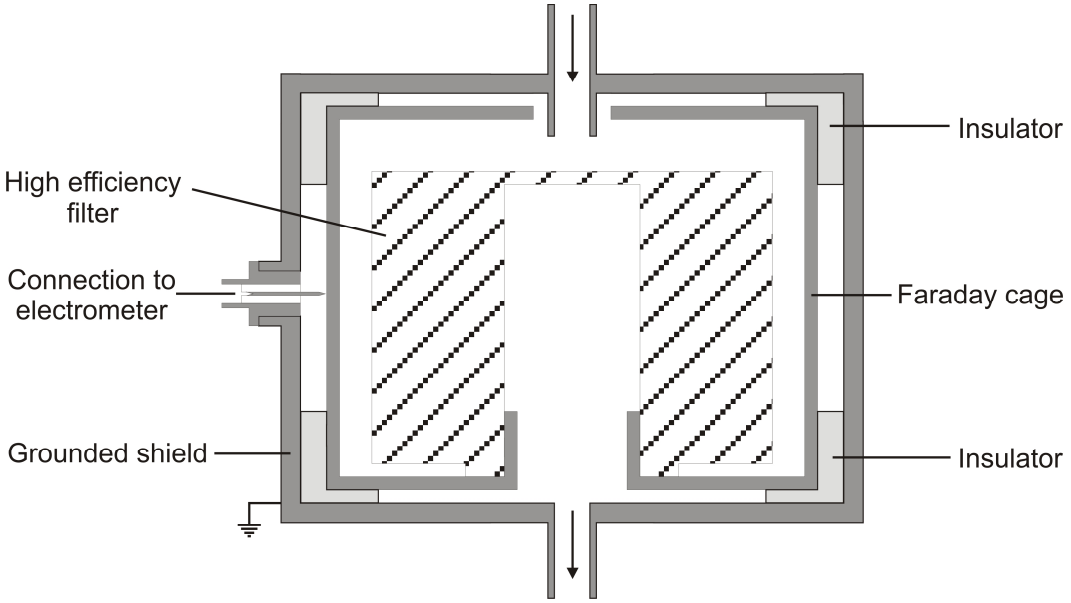

Figure 2. Cross-section of a Faraday cup. Charged particles entering from the inlet are collected by a filter and detected with an electrometer.

Provided that the average charge of the particles (preferably singly charged) and the volumetric flow rate at the inlet are known, the number concentration can be calculated according to the following equation

$$C_{FCAE} = \frac{\Delta I}{Qne\eta_{\mathrm{FCAE}}\gamma}, \tag{1}$$

where ΔI is offset corrected current, Q is the volumetric flow rate of the cup, n is the average charge of the particles, e is the elementary charge, η_{FCAE} is the detection efficiency of the FCAE and γ is the calibration factor of the electrometer. With traceable electric current and flow rate measurements, the number concentration is also traceable. In Eq. 1, the offset corrected current is calculated as

$$\Delta I = I_{particle} - \frac{I_{offset-} + I_{offset+}}{2}, \tag{2}$$

where $I_{particle}$ is the average current induced by the particles. The second term is the average of the two neighboring particle free offset current measurements ($I_{offset-}$ and $I_{offset+}$) which are required in order to eliminate the electrometer background signal current from the results. The flow rate of the cup can be monitored and controlled for example with a mass flow controller (MFC) connected to the exit port. In this case, additional pressure and temperature measurements are required for the inlet port in order to calculate the actual volumetric flow rate at the inlet. As such, the FCAE can be used for calibration purposes at concentrations down to about 1000 particles cm^{-3}, and the device has practically no limitations for the particle size range. Very recently, an FCAE was successfully used as a reference in calibrations at the very low number concentration level of 1 particles cm^{-3} by using an accurate dilution ratio at the inlet of the calibrated instrument (Sakurai and Ehara, 2010; Owen et al., 2012).

Based on the work conducted in Paper I, an example application of this method for a cascade impactor calibration will be given next. In Paper I, the nanoparticle resolution of the ELPI

was improved by designing and manufacturing a new impactor stage (cutpoint 16.7 nm) for the ELPI cascade impactor. The new impactor stage divides the particle size range measured earlier by the filter stage (7–30 nm; Marjamäki et al., 2002) between the new stage and the filter stage. As a consequence, the size resolution was increased in the lower size end of the measured particle size range. This made the instrument more suitable for example for the vehicle engine emission measurements involving nucleation mode particles. The new stage is commercially available as a part of the new ELPI+ impactor, which is an improved version of the original ELPI impactor.

The measurement setup used in the calibration measurements is shown in Fig. 3. In the measurements, polydisperse aerosol distributions were generated from di-octyl sebacate (DOS, density = 0.912 g cm^{-3}) using an evaporation-condensation type aerosol generator presented by Liu and Lee (1975). Because of the small particle sizes to be measured, between 10 and 60 nm, pure DOS was used in the atomizer in order to minimize the changes in particle density caused by the impurities of the solvent. This type of a particle generator is a good choice for calibrations at particle sizes below 100 nm. In this range, the generator is capable of producing fairly narrow size distributions (geometric standard deviation: 1.2–1.4), which is very important in calibration measurements for the reasons that will become clear in the following section.

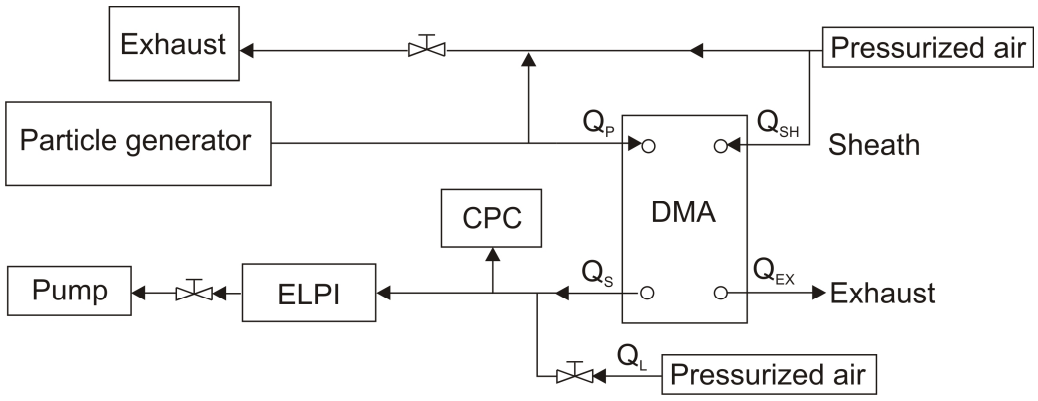

Figure 3. Setup used for the calibration of impactor stages. DMA flow rates: $Q_p = Q_S = 1.5$ L min^{-1}, $Q_{SH} = Q_{EX} = 15$ L min^{-1} (Paper I).

The particle size distribution was measured using a scanning mobility particle sizer (SMPS) consisting of a DMA (TSI model 3085) and a CPC (TSI model 3025A). The same DMA was also used for the selection of monodisperse electrical mobility sizes for the calibration. The electrical current produced by the monodisperse particles was measured with an ELPI from all the impactor stages. Finally, the collection efficiencies for each of the measured particle sizes were calculated as a ratio of the electric current measured from the calibrated stage to the sum of electric currents measured from the calibrated stage and from all the remaining stages in the flow direction, including the backup filter (Keskinen *et al.*, 1999).

The calibration results are presented in Fig. 4 and they will be used as an example in the following section. The results obtained for the individual stages show that the collection efficiency is close to zero for the smallest particles and increases close to 100 % along with an s-shaped curve as the particle size increases. The particle size at which 50 % of the particles are collected is defined as the cutpoint of the stage. Similarly to the collection efficiency of an impactor stage, also the CPC

detection efficiency increases rapidly in the vicinity of the lower detection limit (i.e. cut-off size, size having 50 % detection efficiency). The most common method to characterize the operation of an impactor stage or a CPC is to evaluate the collection efficiency or the detection efficiency curve of the instrument through calibration in the vicinity of the cutpoint or the cut-off size. At larger particle sizes, the instrument response is assumed to be constant (e.g. 100 %), which may or may not be the case depending on the instrument.

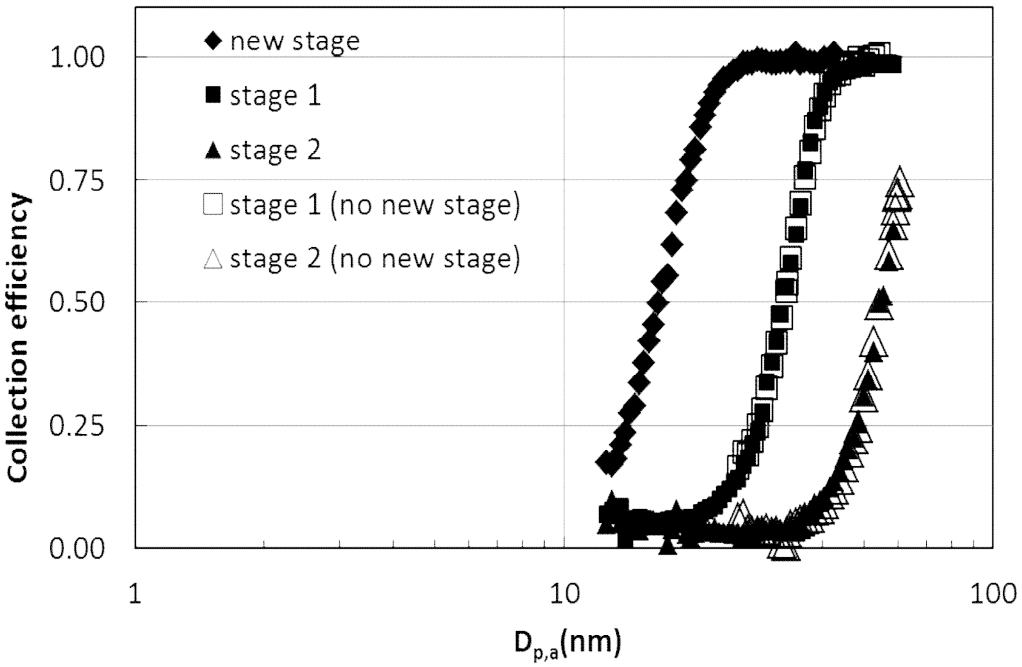

Figure 4. Measured collection efficiency curves for the new impactor stage (leftmost) and for two other stages of the ELPI (Modified from Paper I).

The calibration setup presented in Fig. 3 quite nicely demonstrates that the actual calibration setups are usually more complex than the simplified setup presented in Fig. 1. The complexity is often a result from matching the flow rates and introducing a controlled dilution for the aerosol concentration. In some cases, the measurement system has to be pressurized in order to control the inlet pressure of the instrument. Although the electrical calibration method is fairly easy to use, it has limitations too. As a drawback, this method suffers from the effect of the multiply charged particles, which usually limits the size range of this method. The underlying phenomenon and the means for avoiding this problem will be discussed in more detail in the following section.

3.2. Multiple charge problem

The reasons behind the multiple charge problem are strongly related to the charging of the particles and to the use of a DMA for extracting monomobile particles from a polydisperse size distribution. In Section 2.2, it was stated that the calibration of instruments requires monodisperse particles with a known size and concentration. In the electrical calibration method, there is a strong dependence between these properties. As a rule of thumb, the following applies: if the particles are singly charged, they will also be monodisperse and the FCAE concentration measurement can be conducted accurately by assuming that each particle carries one elementary charge (singly charged

approximation). However, obtaining monodisperse particles with a single elementary charge is not an easy task.

As already stated, particles are brought to a known steady-state bipolar charge distribution (Fuchs, 1963; Wiedensohler, 1988) using for example a radioactive bipolar charger (e.g. *Kr-85* or *Am-241*) before the DMA. This is a very important step, because the original charge distribution of the particles is most likely unknown and the DMA can only classify charged particles of the selected polarity. The resulting equilibrium charge distribution is shown in Fig. 5 for positively charged particles.

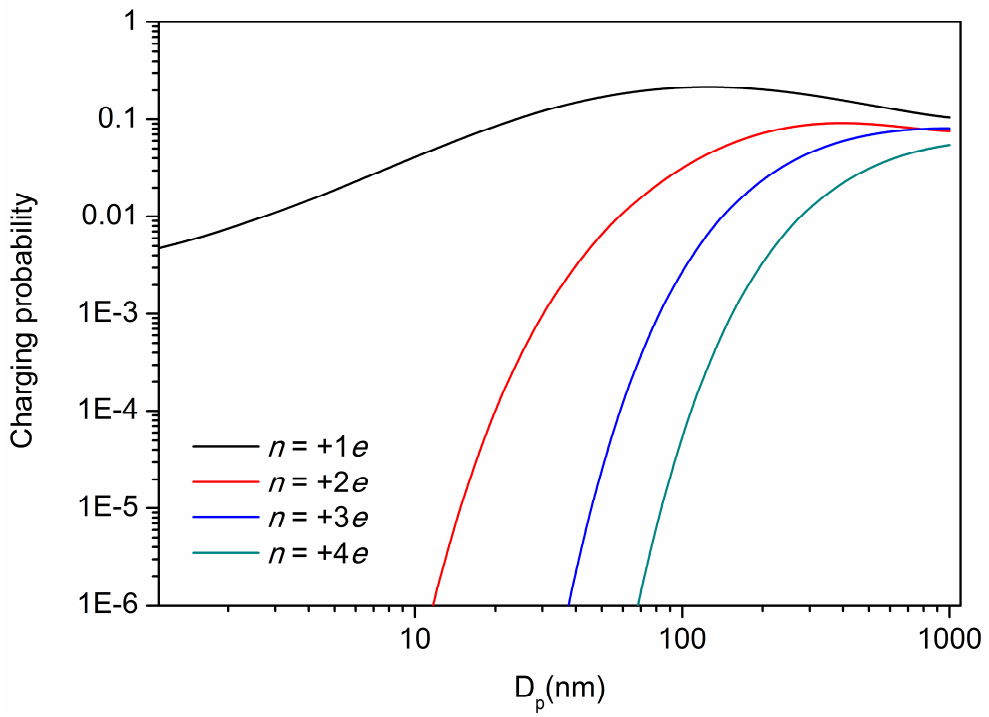

Figure 5. Charging probabilities calculated according to Wiedensohler (1988) for particles having a net charge of plus one, two, three and four elementary charges (e) as a function of particle size.

In Fig. 5, the values in the vertical axis indicate the fraction of particles having n elementary charges from all the particles of the same size. From the DMA's point of view, only the charged particles of the selected polarity (positive in this case) are relevant. The requirement that 99.9 % of the positively charged particles have an equal charge results in an upper limit of approximately 12 nm for particle size. At larger particle sizes, several charging states co-exist in a way that the singly charged particle fraction is always the highest. Instead of the particle size, the DMA classifies particles according to their electrical mobility:

$$Z = \frac{neC_C(D_p)}{3\pi\eta D_p}, \qquad (3)$$

where n is the number of net elementary charges (e) carried by the particle, $C_C(D_p)$ is the particle size dependent slip correction factor, η is the viscosity of the carrier gas and D_p is the mobility equivalent particle diameter. At particle sizes larger than approximately 1 µm, the electrical mobility is directly proportional to n and inversely proportional to D_p ($C_C(D_p) \approx 1$). This means that the particles having sizes D_p and $2 \cdot D_p$ can have the same electrical mobility if they have n and $2 \cdot n$

elementary charges, respectively. This finding applies also for smaller particle sizes. The only difference is that the multiplier between the particle sizes decreases towards smaller particle sizes. Owing to the various co-existing charging states of the particles, the output of the DMA will not be monodisperse in particle size except in two very special and rare cases: 1. The whole particle size distribution lies within the region of uniform charging ($D_p \leq 12$ nm) or the distribution is uniformly charged by other means. 2. The particle size distribution itself is so narrow, that larger multiply charged particles do not exist in the distribution.

Below is an example of a calibration aerosol obtained with a DMA. The geometric mean diameter (GMD) and the geometric standard deviation (GSD) of the original particle size distribution are 100 nm and 1.3, respectively, which are typical for evaporation-condensation type particle generators (Liu and Lee, 1975). For some generators, such as atomizers, nebulizers and the CAST, the geometric standard deviations can be as high as 1.5–1.7.

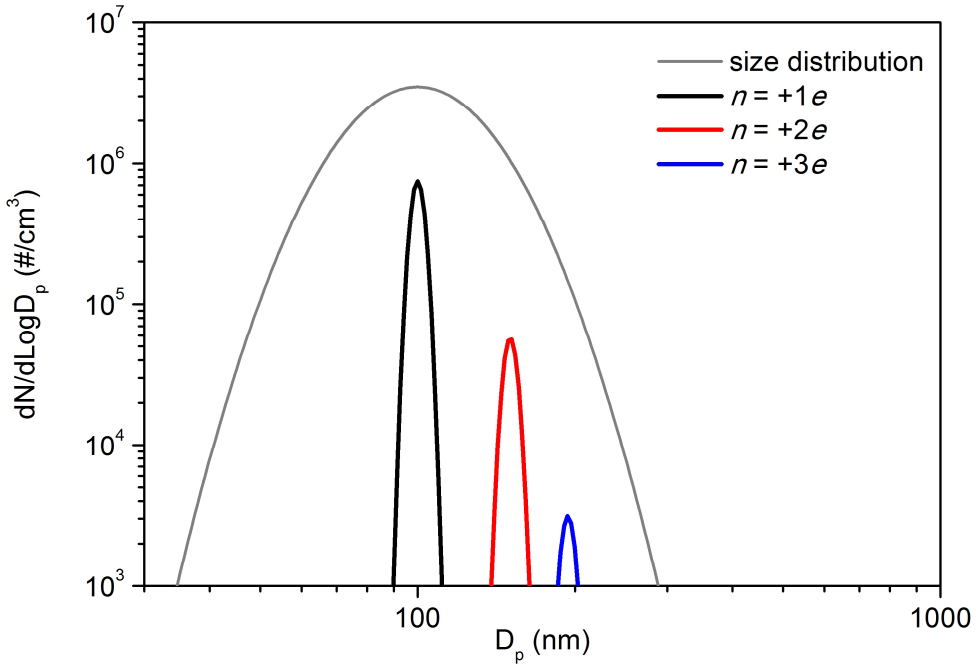

Figure 6. Effect of multiple charging to the output distribution of a DMA. As a DMA is applied for the presented polydisperse size distribution (GMD=100 nm and GSD=1.3), the calibration aerosol will consist of singly, doubly and triply charged particles having different sizes (black, red and blue distributions).

In the case of Fig. 6, 7.5 % of the calibration particles (black, red and blue distributions) have wrong sizes and the use of a singly charged approximation in the FCAE measurement would cause a 14.2 % error to the evaluated reference number concentration. For accurate calibration purposes, not to mention the metrological applications, errors of this magnitude are unacceptable and further actions have to be taken in order to minimize this error. In the case where particle generation characteristics cannot be changed, the simplest way to reduce this error is to carefully select a monodisperse particle size from the right descending edge of the distribution (e.g. Wang and John, 1988; Hillamo and Kauppinen, 1991; Keskinen et al., 1999). This minimizes the concentration of the multiply charged larger particles, but also decreases the measurement signals at the same time. One possibility is to modify the charging characteristics of the charger. In 2002,

Shimada et al. introduced a new type of a bipolar charger using soft X-ray photoionization. In 2005, Okuyama et al. combined the soft X-ray based charging concept with a DMA in order to generate nearly singly charged particles over a wide size range. In their study, the relative fraction of doubly charged particles in the classified aerosol was close to 5 %, which was achieved by adjusting the operating current and voltage of the soft X-ray source.

The fraction of the multiply charged particles can also be minimized by modifying the characteristics of the polydisperse particle size distribution. One way to accomplish this is to apply an impactor stage, with a cutpoint close to the geometric mean diameter of the distribution, for the polydisperse aerosol (e.g. Owen et al., 2012). With this method, the right descending edge of the distribution will become sharper which, combined with a careful selection of the monodisperse particle size, reduces the fraction of multiply charged particles. However, without changes in the flow rate and pressure, the use of a single impactor stage is limited to a very narrow size range, which makes it impractical to use.

Another alternative is to optimize the particle generation in order to produce narrower size distributions. At the National Institute of Advanced Industrial Science and Technology (AIST, Japan), considerable amount of work has been done in optimizing the Electrospray Aerosol Generator (EAG; Chen et al., 1995) based particle generation. Consequently, particularly narrow and stable particle size distributions (GSD $\leq$ 1.15) can be generated in the particle size range between 10 and 200 nm. Thanks to the narrow distributions, fractions even below 1 % are achieved for the multiply charged particles. At AIST, the EAG is used as a part of their primary number concentration standard (Wang et al., 2010; Sakurai and Ehara, 2011).

In most accurate applications, corrections such as presented by Hoppel (1978), Kauppinen and Hillamo (1989), and Takegawa and Sakurai (2011) are applied for the calibration results in addition to the reduction methods presented above. In these correction methods, the particle number concentrations at the output of the DMA are measured for the particle sizes corresponding to singly, doubly and triply charged particles. By applying the charging theories for these concentrations, the fraction of multiply charged particles in the calibration aerosol can be calculated. Provided that measurement data is available for particle sizes corresponding to doubly and triply charged particles matching the singly charged particle size range, the effect of the multiply charged particles can be minimized from the calibration results. These corrections strongly rely on the accuracy of the charging theories and on the accuracy of the particle size distribution or the concentration measurements. Therefore, the corrections are not an ideal solution for the problem. The response of the DUT may also depend strongly on particle size (e.g. Fig. 4) causing iterative correction routines which are sensitive to errors.

In summary although the electrical calibration method is fairly easy to use and the DMA enables particle size selection up to 1 μm, the applicable size range of the method is limited by the multiple charging of particles. In most cases, the calibrations are limited to particle sizes smaller than about 100 nm, which leaves a huge gap between the existing sub-micrometer and micrometer calibration standards. Finding an ideal solution for the problem of multiple charging is highly important, because it would completely solve the calibration issues in the sub-micrometer range.

4. Single Charged Aerosol Reference

4.1. Concept and device

In 2002, Mirme and Tamm presented the novel idea of first charging a nanoparticle size distribution and then growing it to larger size. With this procedure, the charge distribution of the grown aerosol would, ideally, follow the charge distribution of the nanoparticles, i.e. have only a small fraction of multiply charged particles. Recently, Uin et al. (2009) presented a particle generator applying this idea. In the Single Charged Aerosol Reference (SCAR), this novel principle, with some modifications, is combined with a traceable FCAE based number concentration measurement in order to realize a number concentration standard in a wide particle size range. The main development of the SCAR instrument, including designing, building and testing, was conducted at the Aerosol Physics Laboratory of Tampere University of Technology, and is presented in Paper II.

In the SCAR, the following units are used in numbered order to generate narrow, singly charged output aerosol size distributions in a wide particle size range:

1. Generation of primary nanoaerosol
2. Bipolar charging of the primary nanoaerosol
3. Classification of the primary nanoaerosol
4. Condensational growth of the size-classified primary nanoaerosol
5. Traceable FCAE based number concentration measurement from the output

In the first unit, a primary nanoaerosol distribution (GMD 10–12 nm) is generated. In the second unit, the primary nanoaerosol is bipolarly charged according to Fuchs (1963) and Wiedensohler (1988). In the third unit, monodisperse, singly charged particles close to the geometric mean diameter of the primary nanoaerosol are selected with a DMA. In the fourth unit, these particles are grown by the condensation of di-octyl sebacate (DOS) vapour on the particles. The units from 1 to 4 form the enclosed particle generator of the SCAR. Finally, the reference number concentration is measured with a home-built, traceable FCAE in the unit 5, which is connected in parallel with the instrument being calibrated (see Fig. 1).

In Fig. 7, actual measurement data of the primary nanoaerosol distribution and of the size-classified distribution after the DMA is shown together with the charging probabilities for singly and doubly charged particles. The size distributions were measured directly from the SCAR with a nano-SMPS (TSI DMA 3085, TSI CPC 3025A). One of the key parameters which will eventually define the maximum attainable quality for the output aerosol, i.e. how singly charged it will be, is the properties of the primary nanoaerosol. These properties also define the maximum output concentration of the device, which needs to be large enough to be suitable for calibration purposes. In order to produce high quality calibration aerosols, the parameters of the primary nanoaerosol must be carefully selected. In the SCAR, the GMD of the primary size distribution is adjusted to be as large as possible to produce the highest possible output number concentration, but still small enough in order to ensure that the whole primary size distribution lies within the region of uniform charging. This is demonstrated in Fig. 7 and it was already discussed in Section 3.2. As a result, the

fraction of the singly charged particles in the classified primary nanoaerosol should theoretically be 99.975 per-cent. By using these particles as seed particles in the growth unit, it should be possible to grow the aerosol in a way that the particles remain singly charged and that their size distribution remains fairly monodisperse. Provided that this is true, the absolute number concentration of the particles could then be measured accurately with a traceable FCAE.

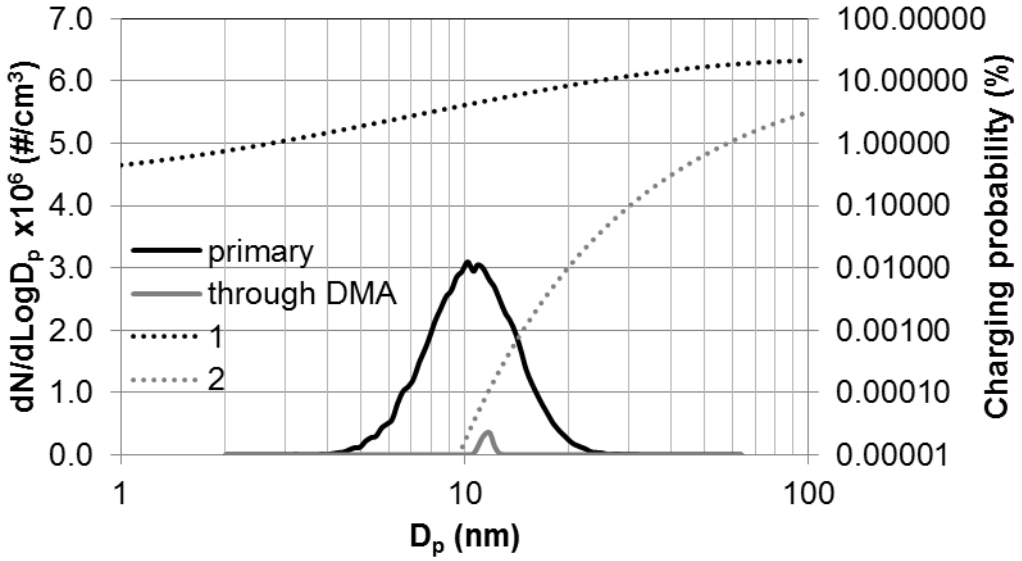

Figure 7. Illustration of the method used in the SCAR-device for producing singly charged, monodisperse seed particles for the growth unit. Primary and through-DMA size distributions are measured with a nano-SMPS from the SCAR. The series 1 and 2 represent the charging propabilities for the corresponding number of elementary charges (Paper II).

Before building the particle generator of the SCAR instrument, a lot of design work was conducted in order to meet the high requirements demanded from an accurate calibration instrument. These included the stability and the repeatability of the output size distribution, which were given a lot of attention in the design phase of the instrument. Also, the SCAR was designed in a way that it allows accurate characterization of all the parameters that were thought to be relevant for the quality of the output. In addition, the objective was to develop a real enclosed instrument instead of a messy table-top construction. This would allow easy transportation of the SCAR, which is needed in order to perform comparisons between the SCAR and other calibration methods, such as performed in the experiments of Paper IV, and also for the planned commercialization of the device. In the end, all these requirements were met satisfactorily, which will become clear by the end of this thesis.

Along with time, two versions of the SCAR have been in use, but never co-existed. The first version of the instrument was a table-top design, which allowed fast modifications, which were required in order to improve the performance of the instrument. This version was only used in the measurements conducted in Paper II, in which the intention was to prove that the SCAR concept works. After the experiments of Paper II, an enclosed version of the particle generator of the SCAR was built mainly by using the components from the first version, but also by introducing some technical improvements. After building the enclosed (i.e. second) version, no mechanical changes have been made. However, the quality of the output has kept improving due to the gained know-

how about optimal operating parameters. The second version of the SCAR has been used in the measurements of Papers III and IV. The continuous development of the SCAR will be reflected in the text while the results of the individual papers are presented.

Next, a more detailed description of the particle generator of the SCAR will be given based on the most recent schematics of the particle generator, which are shown in Fig. 8. The different units of the SCAR are marked using dotted lines. The primary nanoaerosol is generated from NaCl (dissolved in water at 1 g L^{-1} concentration) using an atomizer (ATM 220, Topas, flow rate ~1 L min^{-1}) followed by an evaporation-condensation type generator consisting of a tube furnace (T =900°C, heated length 400 mm) followed by a radial dilution at 10 L min^{-1} flow rate. The inner diameter of the heated quartz glass tube is about 28 mm. According to Bartz et al. (1987), using the atomizer instead of a boat filled with NaCl inside the tube furnace, leads into a very stable aerosol production. With the SCAR, this has also been the case for more than three years now and, therefore, this method has been an excellent choice for the primary aerosol production.

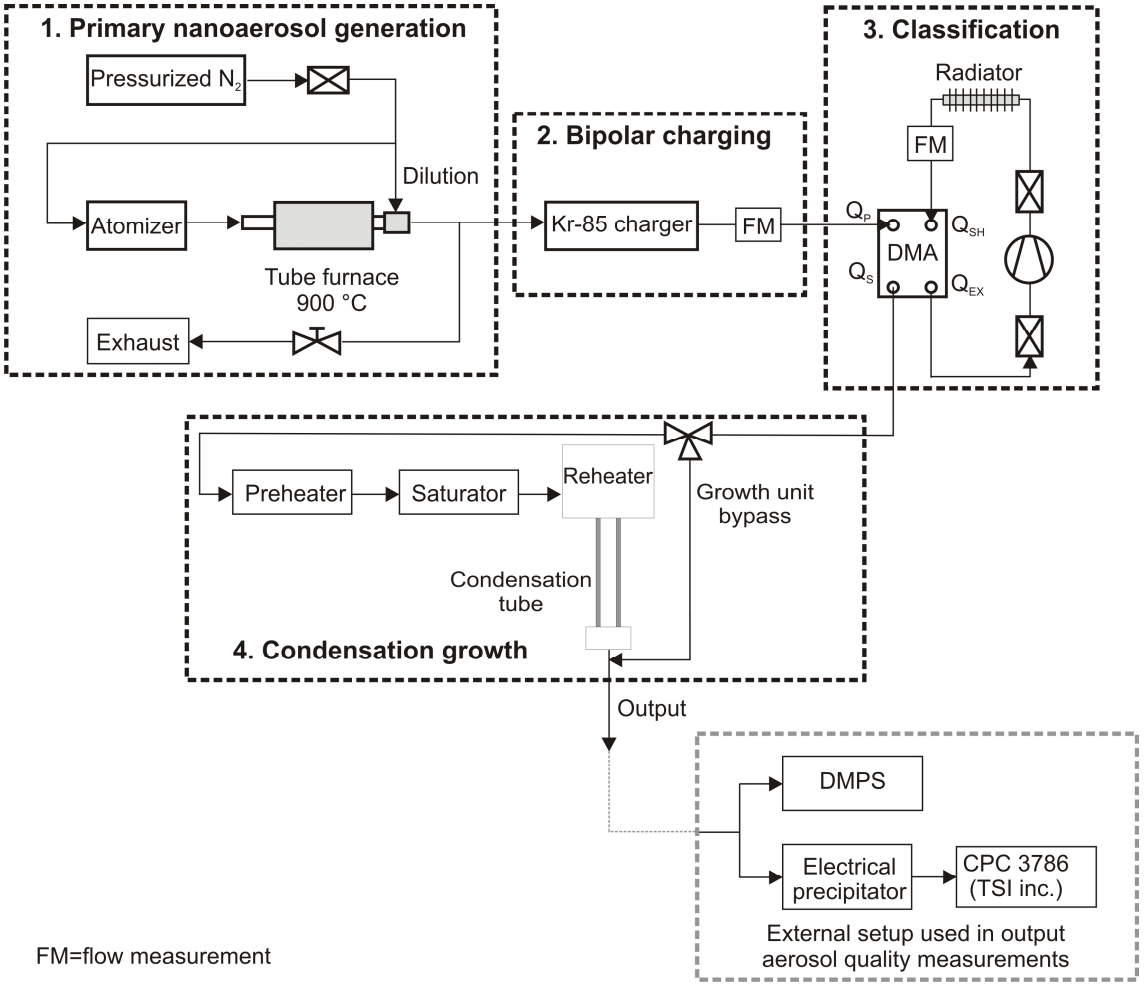

Figure 8. Operational diagram of the SCAR particle generator (Modified from Paper II).

A fraction of the primary nanoaerosol is bipolarly charged with a Kr-85 charger and introduced into the DMA inlet. The inlet flow rate of the DMA is 2 L min^{-1}, which is measured with an orifice, equipped with an absolute and a differential pressure gauge, and adjusted with a control valve located just before the exhaust. The classified aerosol is led through the bypass valve into a

preheater, which ensures that no homogeneous nucleation of DOS takes place at the inlet of a saturator (heated length 140 mm, inner diameter 25 mm). After the saturator, the aerosol enters into a reheater (heated length 200 mm, inner diameter 25 mm, $T = 135°C$), which is followed by a glass tube in which the actual particle growth takes place. The reheater ensures laminar flow conditions for the aerosol before the growth process. The output particle size can be adjusted simply by changing only the saturator temperature in a repeatable fashion, which makes the device very easy to use. Larger particles can be obtained rather rapidly by increasing the saturator temperature. Changing the particle size in the other direction takes somewhat more time because of the heat capacities and the insulation of the components. In the first table top version of the SCAR (used in Paper II), rapid size adjustments were made possible to both directions by using a method similar to the one presented by Ristovski et al. (1998). Later on, this option was removed for simplicity and for better repeatability. In addition to the grown DOS particles, monodisperse NaCl particles up to 30 nm can be generated by using the growth unit bypass and by adjusting the DMA voltage. An actual image of the SCAR is presented in Fig. 9.

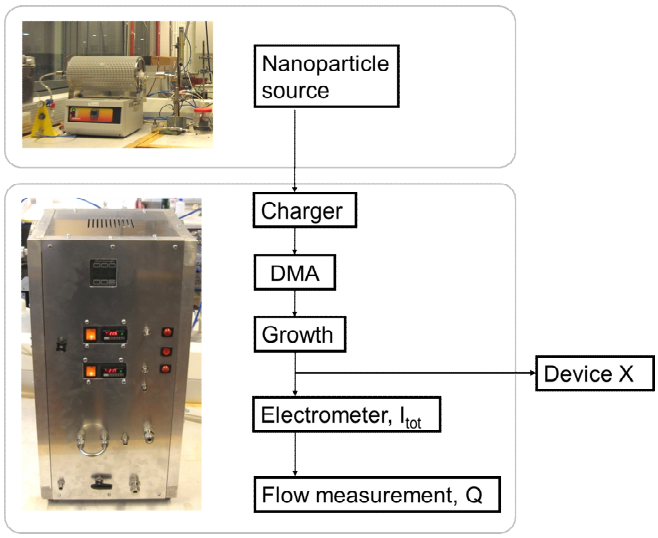

Figure 9. Single Charged Aerosol Reference (SCAR) developed in this thesis.

4.2. Average charge of the output particles

In order to be used as a number concentration reference in calibration measurements of any kind, the quality of the output aerosol has to be studied. To this end, the main task was to assure that the output of the SCAR remains singly charged during the growth process. This was the main objective in Paper II and had a major role also in Paper III. The average charge of particles may change for example because of some unidentified neutralization processes. According to our prior experience, the most probable phenomenon that might affect the average charge of the particles at the output is the homogeneous nucleation of DOS vapor which would produce neutral particles. Also, if some of the particles passed through the growth unit without any significant growth, the coagulation of these small particles with much larger grown particles could increase the fraction of multiply charged particles. These processes are likely to become more and more probable as the aerosol is grown further. Therefore, as the first approximation in Paper II, the fraction of neutral and doubly charged particles in the output was measured for a particle size distribution (mode size 480 nm) located in the upper end of the originally designed operating size range (10–500 nm). The

measurement setup used in the experiments is presented in Fig. 8 together with the particle generator of the SCAR.

The fraction of multiply charged particles was measured with a Differential Mobility Particle Sizer (DMPS), which comprised of a CPC 3025A (TSI Inc.) and a DMA 3071A (TSI Inc.) operated using 0.3/3 (polydisperse/sheath) L min^{-1} flow rates. The fraction of neutral particles was measured with an electrostatic precipitator (ESP) consisting of two concentric cylinders (length 0.7 m, annular slit diameter 3 mm). The ESP was operated at 1 kV voltage and it was followed by a CPC using 0.6 L min^{-1} flow rate. These operating parameters ensured 100 % collection efficiency up to 5 μm singly charged particles. The fraction of neutral particles was evaluated by recording the particle number concentration after the precipitator by switching the HV-source alternately ON and OFF. In order to gain more information about the origin of the neutral particles, the number concentration after the precipitator (HV-source off) was also measured without the primary nanoparticle flow through the growth unit of the SCAR (Paper II). In other words, this means that the operating voltage of the DMA, which is used for obtaining monodisperse seed particles for the growth, was set to zero. In the experiments of Paper III, the particle number concentration at the output of the SCAR was measured with and without the seed particles with an additional CPC. The measurements without the seed particles present the maximum number concentration caused by the homogeneous nucleation of DOS.

Fig. 10 shows the measured number concentration as a function of particle electrical mobility. The mode mobility of the singly charged distribution is denoted as 1 and the respective double and triple mobilities are denoted as 2 and 3. As a result of slightly non-uniform growth conditions after the reheater, a similar tail of the distributions can be identified both from the singly and the doubly charged distributions. Based on the measured mobility distribution, the fraction of doubly charged particles is 0.104%, which is four times larger than the theoretical value calculated from the primary nanoaerosol distribution in Section 4.1 (0.025%). However, in comparison to other devices presented for example by Okuyama et al. (2005) and Uin et al. (2009), who have reported relative fractions of doubly charged particles equal to or less than 5%, our values are exceptionally small. According to the measurements, the maximum fraction of neutral particles in the output aerosol is 0.25%, which can be completely removed by using a secondary DMA if needed. After the precipitator, the same CPC readings were obtained for the neutral particles with and without the condensation nuclei from the SCAR. This gives a reason to believe, that the homogeneous nucleation of DOS dominates the fraction of neutral particles, at least in the upper end of the operating size range of the instrument.

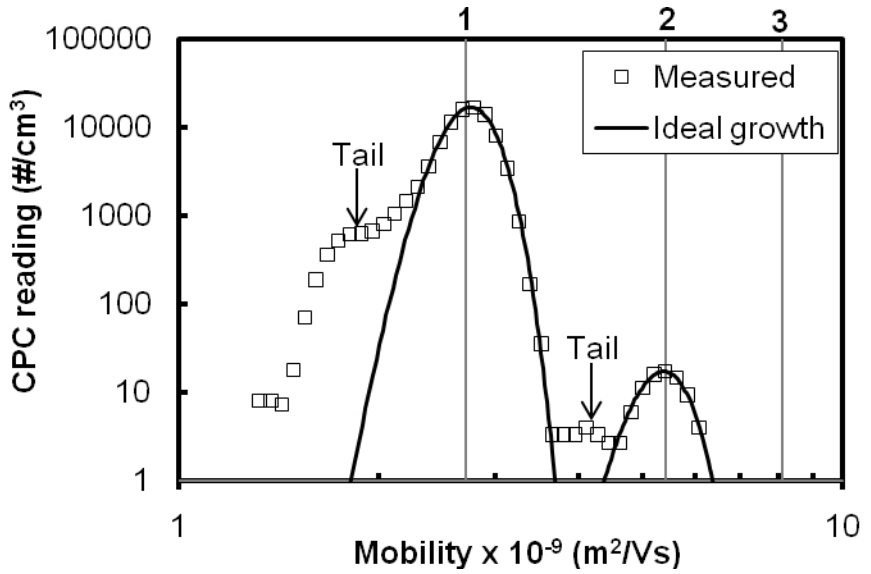

Figure 10. The measured number concentration versus electrical mobility. Vertical lines 2 and 3 denote the locations of the double and triple mobility corresponding the singly charged mode mobility (1) of the distribution. The tail is a result of slightly non-uniform growth conditions in the reheater (Paper II).

Due to the opposite effects of neutral and doubly charged particles, the maximum error caused by the singly charged approximation was estimated to be 0.15%.

In order to be able to assign a reliable uncertainty value for the average charge, a single measurement point clearly is not enough. Therefore, an extensive set of experiments was conducted in Paper III with the setup presented earlier (see Fig. 8) to characterize the fractions of neutral and multiply charged particles and their dependence on operating parameters in the whole operating particle size range of the SCAR. For the fraction of multiply charged particles, the varied initial parameter was the GMD of the primary nanoaerosol distribution. In these measurements, two GMD values (11 nm and 12 nm) were used and the monodisperse particle sizes for the growth were selected from the peaks of the distributions. As suspected, the results indicated that the fraction of multiply charged particles increases at all particle sizes as the GMD increases. For neutral particles, the varied initial parameter was the input concentration of the particles entering into the growth unit. For this experiment, the main result was that the fraction of neutral particles decreases with increasing input concentrations. As such, these results may not seem so important but, combined with the size responses of these fractions, they can be used effectively for evaluating the uncertainty of the average charge. The size responses for the multiply charged particles at the two mentioned GMDs and a typical size response for neutral particles are shown in Fig. 11. The results indicate that the both fractions increase with increasing particle size and that neither of the fractions is zero at the lower end of the measured size range.

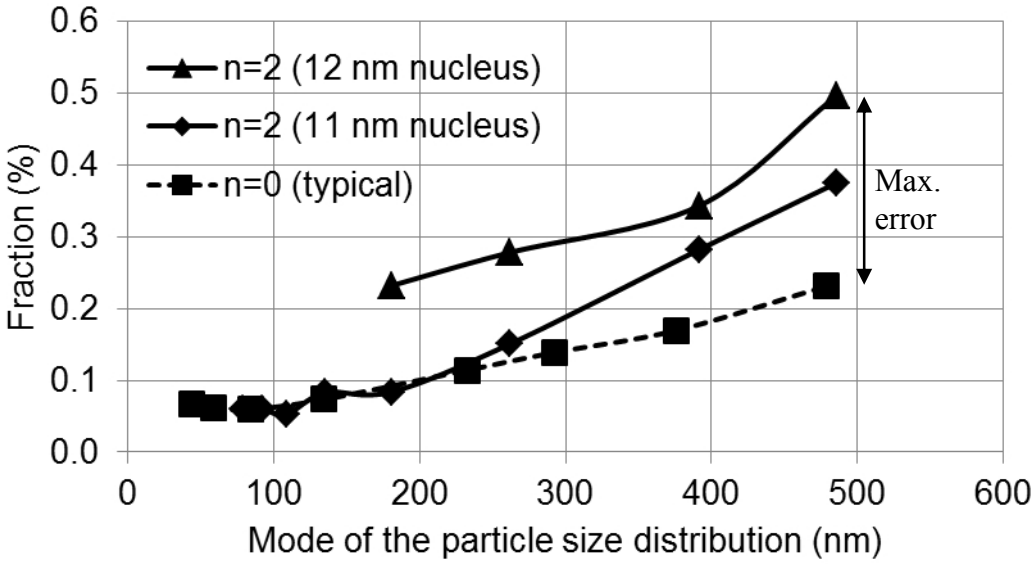

Figure 11. Fraction of doubly charged particles (n = 2) for 11 and 12 nm primary nanoparticles together with a typical case for neutral particles (n = 0) as a function of the output particle size. The maximum error caused by the combined effect of multiply charged and neutral particles is denoted with a vertical line (Modified from Paper III).

As the basis of the uncertainty evaluation, it is assumed that the calibration measurement for a single particle size takes no more than one hour, which is true for the SCAR. During this period of time, the stability of the primary nanoaerosol distribution is of particular importance and needs to be proven. In Paper III, it was demonstrated with measurements that the GMD of the primary nanoaerosol distribution changes only about 0.3 nm during two hours of continuous operation. This means that the GMD can be easily adjusted in a way that it remains between 10 and 12 nm during the calibration measurements. Therefore, the results for the 12 nm primary nanoparticles can be used as the upper limit for the fraction of multiply charged particles. Because of the opposite effects of the multiply charged and neutral particles, the associated error equals to the difference between these fractions. Taking the worst case for the multiply charged particles and a typical case for the neutral particles and selecting the largest particle size from the results in Fig. 11, the maximum error is found to be 0.27 %. By assuming a rectangular probability distribution (i.e. all values between 0 and 0.27 % are equally probable) for this error, 0.16 % standard uncertainty is obtained for the use of singly charged approximation with the SCAR. This applies to the whole operating particle size range. The fact that the output aerosol of the SCAR remains singly charged in the whole operating particle size range is the single most convincing proof of the operation of the SCAR concept. It also suggests that, combined with a traceable FCAE based number concentration measurement, the SCAR can be used for performing accurate calibrations of various instruments which measure the number concentration of particles. This has been proven by experiments in Papers III and IV.

Even though the fractions of multiply charged and neutral particles are exceptionally small and their contribution to the overall accuracy of the SCAR is negligible, the sources of these fractions need to be discussed. In Fig. 12, measurement results for the fraction of neutral particles are shown with and without the seed particles. The latter one is calculated as a ratio of the output number concentration obtained without the primary nanoparticles to the output number

concentration obtained with the primary nanoparticles. The results without the primary particles demonstrate that the neutral particle fraction is dominated by homogeneous nucleation in the upper end of the measured size range. Quite interestingly, this is not the case for particle sizes up to about 400 nm. Up to this size, the results without the primary nanoparticles show much smaller neutral particle fractions than the measurements with the primary nanoparticles. This gives a reason to believe that the neutral particles are, in fact, formed by some kind of an unidentified neutralization process.

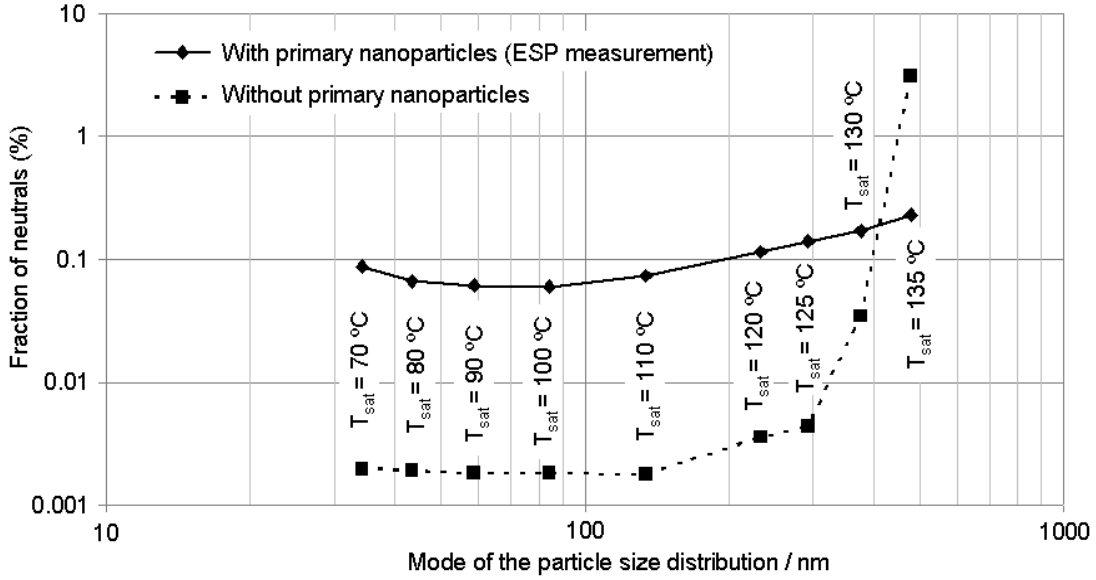

Figure 12. Fraction of neutral particles ($n = 0$) as a function of the output particle size measured with and without the primary nanoparticles (Paper III).

The cause for this neutralization of the particles has not been identified in any of the publications dealing with the SCAR. However, the following hypothesis might be worth testing: could the cause for the neutralization simply be the fact that, in the enclosed SCAR particle generator, the *Kr-85* neutralizer is located relatively close to the preheater, the saturator and the reheater? This may create an ion concentration inside the mentioned parts which, if sufficient, could cause changes to the net charge of the particles. Another possibility is that the neutralization is caused by the high temperatures inside the SCAR, which may be difficult to prove. Unfortunately, these hypotheses have not yet been tested experimentally.

4.3. Operating size and concentration ranges

In the calibration measurements performed with the SCAR, the intention is to use the whole output particle size distribution as a calibration aerosol, provided that the aerosol can be trusted to be singly charged ($D_p \leq 500$ nm). In Section 2.2, it was stated that the calibration measurements generally require monodisperse calibration aerosols. In order to meet this requirement, the output size distribution should remain fairly narrow (GSD ≤ 1.3) during the growth process. This was taken into account already in the design phase of the SCAR by using monodisperse seed particles as a starting point and by paying attention to the design of the growth section of the instrument. During the work conducted in Papers II and III, the characteristics of the output particle size

distribution were studied extensively by using an SMPS and a CPC for particle sizes up to 500 nm. As a result of Paper IV, the characterized size range was extended up to 1 μm.

Fig. 13 shows five different output size distributions measured with an SMPS directly from the output of the SCAR. The leftmost distribution presents the classified primary nanoaerosol size distribution without any growth. For the rightmost size distribution, a log-normal fit function has been applied for the SMPS measurement result, because of the limited size range of the SMPS.

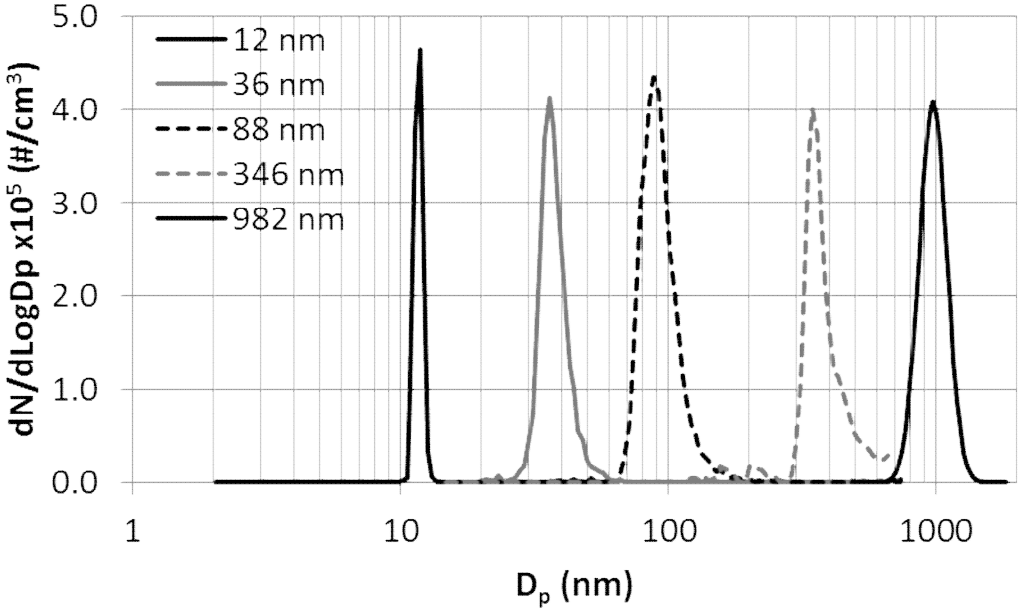

Figure 13. Examples of the SCAR-device output particle size distributions measured with an SMPS. The corresponding mode sizes are shown in the legend (Modified from Paper II).

According to the measurements, the grown distributions are somewhat wider than the distribution of the 12 nm seed particles, but fairly narrow particle size distributions up to 1 μm can be produced. Based on the CPC number concentration measurements, the output number concentration vary only slightly as a function of the particle size, which has been presented in Paper II. A thorough description of the properties of the output aerosol is presented in Table 1. The number concentration range at the output extends from 0 particles cm^{-3} up to the maximum value of about 60 000 particles cm^{-3}, which is sufficient to cover most of the measuring concentration ranges of commercial CPCs. The SCAR particle generator is operated in a way that the aerosol flow inside the generator is always kept constant at 2 L min^{-1}. At larger output flow rates, the output number concentration starts to decrease as the aerosol begins to dilute. With the current setup, output flow rates up to 20 L min^{-1} can be produced.

In actual calibration measurements, the SCAR can be used in two different setup configurations (see Fig. 17). The configurations result in three different operation modes, each having its own operating size range. By using the growth unit bypass (see Section 4.1), monodisperse NaCl calibration aerosols can be produced (Mode 1, setup I). By using the growth unit, fairly narrow, singly charged DOS calibration aerosols can be produced up to 500 nm in particle diameter (Mode 2, setup I). These two methods do not require any changes to the experimental setup. The third operation mode is related to the fact that, at 1 μm, the output aerosol contains a substantial fraction of neutral particles. This problem can be solved by using a secondary

DMA at the output of the SCAR (Mode 3, setup II, Fig. 17). Thus, genuinely singly charged particles can be produced up to 1 μm, at the expense of a decreased output number concentration (≤ 10 000 particles cm^{-3}). Regardless of the operation mode, the GSD of the output aerosol size distribution remains below 1.3 in the whole operating size range, which is important in the calibration measurements.

Table 1. Characteristics of the output aerosol of the SCAR.

Number concentration	~ 60 000 particles cm^{-3} (max.)*
Electric current	~ 500 fA (max.)*
Sample flow	0–20 L min^{-1}
particle size range	NaCl: 10–30 nm, down to 3 nm at lower concentrations DOS: 30–500 nm, up to 1 μm with an additional DMA
GSD	1.03–1.30 depending on the particle size
Particle density ($D_p \geq$ 30nm)	0.91 g cm^{-3} (DOS)

*Valid up to 2 L min^{-1} output flow rate

4.4. Stability and repeatability of the output aerosol

In Section 4.2, it was stated that calibration measurement for a single particle size can be performed within one hour by using the SCAR. During this period of time, the primary nanoaerosol distribution was required to be stable in size, because the changes in the size would directly affect the quality of the output aerosol. Similarly, also the size of the output distribution itself should remain stable during the calibration measurements. Although this has been verified during the measurements reported in each and every one of the related publications, it has never been presented. Unlike the stability, the repeatability of the output from day to day was demonstrated in Paper III. It was shown that, independently from the output concentration and the measurement day, the output particle size can be predicted with 5 % accuracy with a polynomial fit based only on the temperature setting of the saturator. Fig. 14 shows an example of the SMPS measurement results for the mode of the output particle size distribution during a one hour long continuous calibration routine for two different output particle sizes. The datasets have been taken from the measurements conducted in Paper IV. The calibration routine consisted of four sections, including two sections for adjustments, stabilization and configuration changes, and two for performing the actual calibration measurements in the configurations *a* and *b*. By comparing the nominal calibration particle size with the actual measurement data, it can be seen that the output aerosol is very stable in time. In fact, a closer look at the data reveals that the variation of the mode size is smaller than the size resolution of the SMPS measurement.

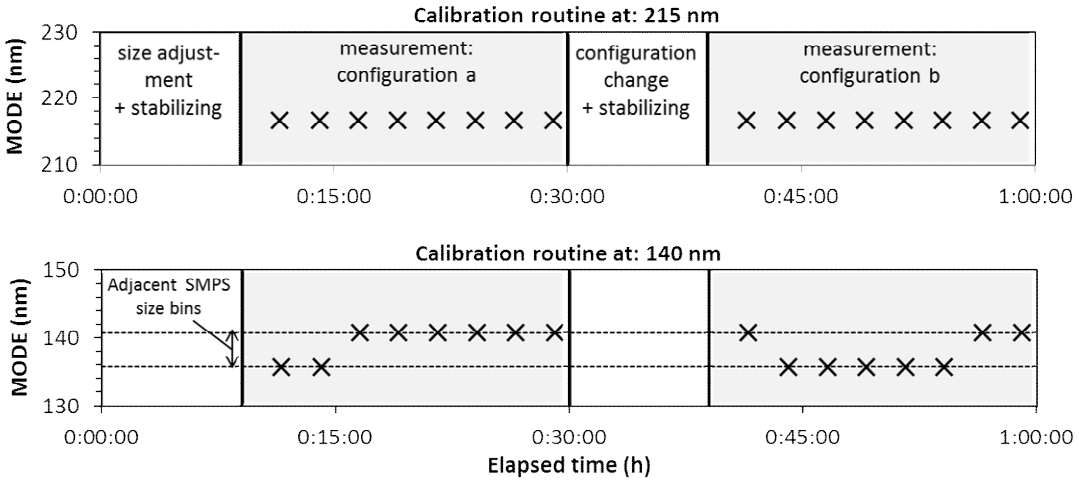

Figure 14. Stability of the output aerosol during a one hour long calibration routine for two different particle sizes. The data points present the modes of the SMPS size distribution measurements and are taken from the experiments of Paper IV. The measurement routine consisted of four sections which are discriminated using vertical lines and different background color.

So far, it has been proven that the particle generator of the SCAR operates in a stable manner. In the calibrations conducted using the SCAR, the particle size of the calibration is in most cases measured with an SMPS which is connected in parallel with the FCAE and the DUT. In parallel measurements, the delay times of the sampling lines may be different. This means that, in the case of liquid (DOS) particles, the size input for the two measurements may be different because of the evaporation of the particles. The same applies also for the electrical calibration method (see Section 3.1) if the particles have a long residence time in the sampling line between the DMA and the concentration measurement. Whether this is a problem with the SCAR, depends on the properties of DOS, on the particle size and on the difference between the delay times. The evaporation of common liquid calibration aerosols, such as di-octyl phthalate (DOP) and DOS has been studied experimentally for example by Rader et al. (1987). In their study, freshly generated monodisperse aerosol particles were allowed to evaporate inside a laminar flow evaporator (i.e. a metal tube) having a residence time of somewhat more than 100 seconds. The rate of evaporation was studied by measuring the particle size before and after the evaporator. They found that, in general, DOP particles evaporate more easily than DOS particles. They also demonstrated that the changes in the respective diameter for initially 40 nm and 30 nm DOS particles were about 10 % and 24 %, which are noticeable changes. These results do not directly apply for the SCAR, because a residence time of 100 s is much longer than the expected maximum difference in the delay times using the SCAR. Nevertheless, they indicate that the evaporation of DOS particles might be possible also with the SCAR.

Motivated by the study of Rader et al. (1987), the evaporation of the DOS particles was studied at particle sizes between 10 nm and 60 nm. Within this size range, the following simplified equation can be used for calculating the rate of evaporation (or condensation)

$$\frac{d\left(D_p\right)}{dt} = \frac{2M\alpha_c\left(p_\infty - p_d\right)}{\rho_p N_a \sqrt{2\pi mkT}} = \frac{2M\alpha_c\left(p_\infty - p_s \cdot \exp\left(\frac{4\sigma M}{\rho_p RTD_p}\right)\right)}{\rho_p N_a \sqrt{2\pi mkT}}. \quad (4)$$

In Eq. 4, M, m, ρ_p and σ are the molecular weight, mass of a molecule, density and surface tension of the evaporating liquid, respectively, which can be found from common references such as Hinds (1998). α_c is the condensation coefficient and N_A, k and R are natural constants. Similar to the experiments of Rader et al. (1987), we performed our calculations at room temperature (T = 298.15 K), which is the normal output temperature for the SCAR. In order to evaluate the maximum effect of evaporation, the vapor pressure far from the particles, p_∞, was assumed to be zero. An estimation for the saturation vapor pressure over a flat surface in Eq. 4, p_s, was obtained by reproducing the experimental results of Rader et al. (1987). This resulted in the value of $6.0 \cdot 10^{-5}$ Pa for the vapour pressure.

Fig. 15 shows our simulation results for the evaporation of liquid DOS particles.

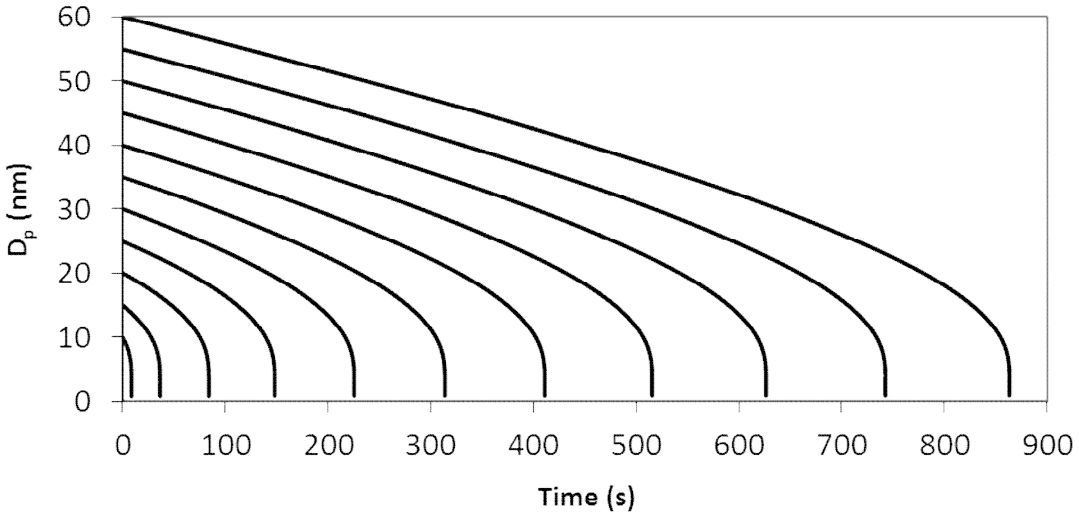

Figure 15. Evaporation of liquid DOS particles having initial sizes between 10 nm and 60 nm at room temperature. The saturation vapor pressure without the Kelvin effect is $6.0 \cdot 10^{-5}$ Pa and the vapour pressure far from the particles is zero.

According to the results, evaporation times in the studied size range are between 8.8 s and 863 s, and, at all sizes, noticeable size changes can be observed already at the beginning of the evaporation process. From the calibration point of view, perhaps the most relevant question is the following. If a certain percentage diameter change (i.e. error) is allowed between the size and concentration measurements and the smallest particle size to be measured is D_p, what is the maximum allowed difference in the delay times which satisfies these conditions? Answer to this question was calculated from the results shown in Fig. 15 and is presented in Fig. 16. Each line in Fig. 16 presents the evaporation time required for a constant percentage diameter change as a function of the initial particle diameter. The usage of the data in Fig. 16 is best described with an example case, in which the SCAR is used. For the SCAR, the smallest DOS particle size to be measured is 30 nm, to which a 1 % error caused by the evaporation is allowed. By selecting the line that represents the 1 % diameter change (bolded line) from Fig. 16, and by selecting the 30 nm size, the maximum allowed difference between the delay times can be read from the y-axis. As a result, a 5 s difference

is obtained. With the SCAR, the difference can always be expected to be smaller than 2 s, which means that particle sizes down to about 20 nm can be measured reliably.

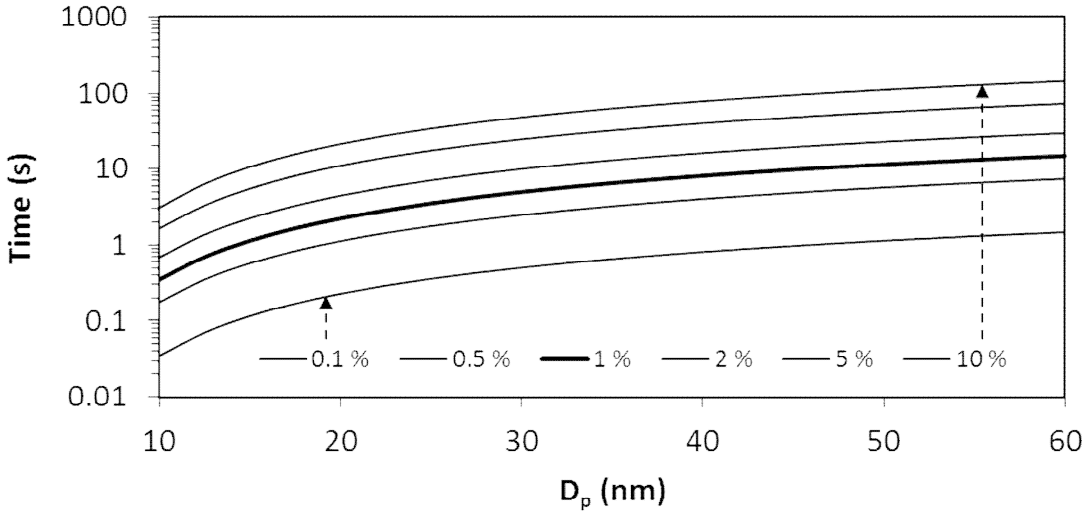

Figure 16. Evaporation time required for a constant percentage diameter change as a function of initial particle size. Each line represents a different constant percentage change, as denoted by the legend. The lines are calculated from the results presented in Fig. 15.

4.5. Uncertainty of the output number concentration

The main function of a standard is to provide traceability and accuracy for measurements. Therefore, the number concentration output of the SCAR should provide traceability to primary realization of the SI units and to have the highest attainable accuracy, i.e. to have the smallest possible uncertainty. In an FCAE based number concentration measurement, the overall uncertainty is determined by the component uncertainties of the quantities that are needed for calculating the number concentration (Eq. 1). That is, the uncertainty of the volumetric flow and electric current measurements, the uncertainty of the average charge of the particles (n) and the uncertainty of the detection efficiency of the Faraday cup (η_{FCAE}). For the SCAR, the traceability was established as a part of a careful validation process conducted in co-operation with Mikes–Centre for Metrology and Accreditation (Finland) in Paper III. During this process, the FCAE of the SCAR was equipped with traceable, high-quality electric current and volumetric flow sensors. These sensors were carefully calibrated at Mikes (see Paper III for the standard uncertainties), which guaranteed the best available accuracy for the measurements. The uncertainty of the average charge of the particles has already been presented earlier in Section 4.2. Based on the results, it can be said that, with no doubt, the uncertainty of the average charge will only have a minor contribution to the overall uncertainty. In actual measurements, a constant value (1.0000) is used for the average charge of the particles and a 0.0016 standard uncertainty is associated to it.

The Faraday cup of the SCAR is a result of an extensive amount of design and experimental work. For a Faraday cup, the most important property which eventually defines the attainable measurement accuracy is the detection efficiency. The use of a filter having a collection efficiency value above 99.99 % at all particle sizes is a good starting point, but it does not guarantee

high detection efficiency for the cup. In a well-designed Faraday cup, the η_{FCAE} can be calculated as a product of the diffusion limited particle penetration through the inlet tubing and the collection efficiency of the filter, which is the case with the SCAR (see Fig. 2). In practice, this means that the inlet tube transports the aerosol directly inside the Faraday cage. In a poorly designed Faraday cup, particle losses caused by diffusion and inertial effects may occur in other parts of the Faraday cup as well. For the Faraday cup of the SCAR, the collection efficiency of the filter is above 99.99 %. Therefore, a constant value (1.000) is used for the collection efficiency with 0.001 standard uncertainty. The diffusion losses at the inlet tube are minimized by making the tube as short as possible (length 4 cm). The diffusion limited penetration is calculated according to Gormley and Kennedy (1949) and the associated standard uncertainty is calculated assuming a symmetric, rectangular probability distribution with a half width of 20 % of the losses (i.e., 1 - penetration).

In addition to the uncertainties presented above, the uncertainty of the output number concentration is affected by the random noise of these components (type A uncertainties) during the actual concentration measurement. In general, the contribution of the random noise to the overall uncertainty decreases with increasing measurement time. For a certain measurement time, the contribution of the random noise can be minimized by finding out the optimal measurement routine. Another important requirement for a good measurement routine is that the data which it provides enables reliable determination of the uncertainty caused by the random noise. In order to accomplish this, several repetitions for each measurement point are needed. The measurement routine used with the SCAR has been continuously developed, leading to smaller and smaller uncertainties for the output. The uncertainty of the output number concentration is an integral part in the evaluation of the CPC detection efficiency and its uncertainty. For consistency, the whole evaluation process, together with the most recent measurement routine, will be presented in the next chapter.

Without going into the details of the uncertainty analysis, Table 2 shows in a simplified manner how the overall uncertainty of the output number concentration is formed from individual uncertainty components. In the calculation of the overall uncertainty, the individual uncertainty components are treated as uncorrelated quantities. The values in Table 2 represent a typical case for the output of the SCAR. Based on the results, the overall uncertainty of the output number concentration is about 1.3 %. This uncertainty is mostly caused by the uncertainties in the electric current and volumetric flow measurements. The uncertainties of the FCAE detection efficiency and the average charge of the particles have only a minor contribution to the overall uncertainty.

Table 2. Typical values for the component uncertainties and their contribution to the overall standard uncertainty of the output number concentration. Results apply in following conditions: number concentration, 9000 particles cm^{-3} ; FCAE flow rate, 1.5 L min^{-1} (Modified from Paper III).

Source of uncertainty	Contribution cm^{-3}	%
Electric current	105	1.16
Volumetric flow rate	45	0.50
Average charge of particle	14	0.16
FCAE detection efficiency	9	0.10
Overall uncertainty	115	1.28

5. SCAR as a primary number concentration standard

5.1. Experimental setup and calibration routine

In this section, the most recent experimental setups and the calibration routine will be presented through an example CPC calibration, which was conducted in Paper IV. In the experiments of Paper IV, the SCAR was applied for the calibration of a CPC 3772 (TSI Inc.) between 10 nm and 1 μm, by using a completely new measurement routine. The new routine improved the overall accuracy of the SCAR remarkably. Before getting into the details of the experimental setup, a few general remarks considering the calibration of instruments (e.g. CPCs) are in order. In general, the most important function of a calibration, at least from the end user's point of view, is that it represents the operation of the instrument in conditions of the intended use of the instrument. For an aerosol instrument, these conditions include particle material (e.g. liquid or solid), particle size, number concentration and ambient conditions such as pressure and temperature. For the smallest of all particles (size close to 1 nm), the charge of the particles used in the calibration may also be important. In an ideal calibration, all of these conditions correspond to the actual operating conditions of the instrument. For practical reasons, calibrations are often conducted in normal laboratory conditions (temperature ≈ 25 °C, pressure ≈ 101 kPa), which is also the case for the SCAR. In a versatile calibrator, other conditions, such as particle size and concentration, can be altered within a wide range, without major modifications to the calibration setup.

Fig. 17 shows the experimental setups that are used with the SCAR in calibration measurements.

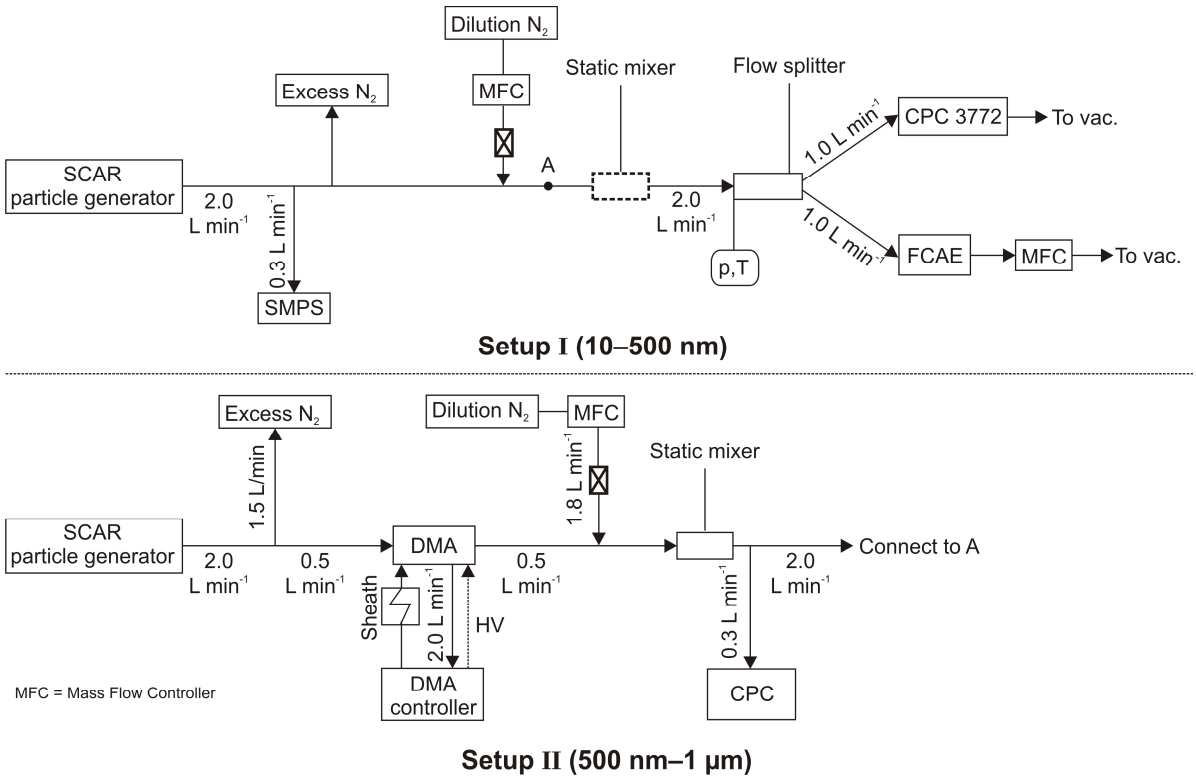

Figure 17. Measurement setups used with the SCAR in a CPC calibration (Paper IV).

The setup I in Fig. 17 is the normal configuration of the SCAR in which the whole output aerosol size distribution is used as a calibration aerosol (see Section 4.3). With this setup, calibration measurements can be performed at particle sizes from 10 nm up to 500 nm and the mode of the output particle size distribution is used as the particle size of a calibration. The output particle size distribution just downstream of the particle generator (i.e. the particle size of the calibration) is measured using an SMPS. The particle size measurement is conducted simultaneously with the CPC and FCAE number concentration measurements. In the example case presented in Fig. 17, the SMPS consists of a TSI 3081 DMA connected to a TSI 3080 controller and a TSI 3775 CPC, but others can be used as well. As mentioned earlier in Section 4.3, the internal flow rate of the particle generator is always 2 L min^{-1}. The particle number concentration is controlled by changing the flow rate of the dilution nitrogen, which controls that fraction of the 2 L min^{-1} aerosol flow which escapes to the excess port. Based on the results in Paper IV, a static mixer was added to the setup in order to guarantee the homogeneity of the particle flow before the flow splitter. The CPC and the home-built Faraday cup sample the aerosol simultaneously downstream the flow splitter at the nominal volumetric flow rate of the CPC. Having equal flow rates at different output branches of the flow splitter is very important because unequal flow rates may lead to different number concentration inputs for the instruments. The inlet flow rate of the Faraday cup is controlled with a mass flow controller (Model F-201CV-10K-RAD-33-V EL-FLOW by Bronkhorst). In order to convert the mass flow rate to volumetric flow rate at the inlet of the Faraday cup, both pressure (Model PTB 330, Vaisala) and temperature (Model H2081 NPT thermistor probe with stainless steel sheath, US Sensors) are measured before the flow splitter. The electric current from the

Faraday cup is measured using a Keithley 6430 sub-femtoamp remote sourcemeter. At particle sizes between 500 nm and 1 μm calibrations are conducted by using the setup II in Fig. 17. In this setup, a DMA is connected to the output of the SCAR in order to ensure singly charged aerosol for the calibration. In calibration measurements, the same DMA is used both for the particle size distribution measurement (together with a CPC) and for selecting the monodisperse particle size for the calibration.

With both setups, the measurement routine that is used in AIST in CPC calibrations (e.g. Sakurai and Ehara, 2011) is used for acquiring the CPC and FCAE readings. For convenience, its application will be first explained for the setup II. While the CPC and FCAE are recording the concentration and current, the DMA voltage is toggled *on/off* every 60 s. Consequently, the number concentration input for the CPC and the FCAE during each 60 s period is either zero (DMA voltage *off*) or equals the calibration number concentration (DMA voltage *on*). The toggling is repeated without interruptions until 10 measurement cycles (*off-on-off*) are produced. Thus, the total measurement time is 21 min: 11 *off* periods and 10 *on* periods. An estimate for the actual particle concentration during a single measurement cycle is then calculated by subtracting the average value of the two neighboring *off* periods from the *on* period concentration as presented in Eq. 2. After the DMA voltage is toggled, the instruments need some time to stabilize. Therefore, in each of the 60 s periods, the average values are calculated by using data only from the last 30 s. As a result, 10 values in total are obtained both for the average concentration measured by the CPC and for the average concentration measured by the FCAE. After completing the measurement routine presented above, the places of the FCAE and the CPC are switched and the routine is repeated, which ends the measurements for a single particle size.

In the setup I in Fig. 17, a different method has to be applied for producing the *off* and *on* periods due to the absence of the DMA. In this setup, the particle concentration input for the CPC and the FCAE is toggled between zero and the actual calibration concentration by toggling the flow rate of the dilution nitrogen between two different values. A value higher than 2 L min^{-1} results in zero concentration for the instruments and a smaller value is used for producing the actual calibration concentration. With the SCAR, measurements for a single particle size, including size, concentration and configuration changes, can be completed within one hour. Although this measurement routine may at first sight seem quite heavy, it has many advantages. Among other things, it provides a lot of data (many repetitions), which makes the uncertainty evaluation for the detection efficiency much easier and more reliable.

5.2. Evaluation of the CPC detection efficiency and its uncertainty

The following procedure for calculating CPC detection efficiency and evaluating its uncertainty is applicable to measurements conducted using the measurement routine presented in the previous section. The uncertainty of particle size is not taken into account in the evaluation process. The procedure itself was developed and presented in Paper IV, and was applied to the detection efficiency measurements conducted with the SCAR and with the primary NCS of AIST. In Paper IV, special attention was paid to the uncertainty evaluation process. The presentation below follows the presentation in Paper IV.

In general, the detection efficiency is defined as a ratio of the number concentration measured by the CPC to that measured by the FCAE:

$$\eta_{CPC} = \frac{C_{CPC}}{C_{FCAE}}, \tag{5}$$

where C_{CPC} and C_{FCAE} are the average concentrations of ten repetitions. This equation results in the true detection efficiency value only in a special case, in which the number concentration inputs for the two instruments are equal. The difference between the input concentrations is usually referred as the bias (β). The bias is defined as follows: let C_1 and C_2 be the number concentrations at two fixed output branches of the flow splitter, denoted as sampling ports 1 and 2, to which the CPC and the FCAE are connected in the original configuration, respectively. The bias between the sampling ports is defined as the ratio of the respective input concentrations

$$\beta_a = \frac{C_1}{C_2}. \tag{6}$$

The effect of the bias can be eliminated from the results as follows: first, the detection efficiency is measured in the original configuration. Then, the places of the CPC and the FCAE are switched and another efficiency measurement is conducted in the switched configuration. The two efficiency measurements result in the following equations for the concentration biases. For configuration *a* (original):

$$\beta_a = \left(\frac{C_1}{C_2}\right)_a = \frac{C_{CPC} / \eta_{CPC}}{C_{FCAE}} = \frac{\eta_a}{\eta_{CPC}} \tag{7}$$

and for configuration *b* (switched)

$$\beta_b = \left(\frac{C_1}{C_2}\right)_b = \frac{C_{FCAE}}{C_{CPC} / \eta_{CPC}} = \frac{\eta_{CPC}}{\eta_b}, \tag{8}$$

where η_a and η_b are the average detection efficiency values calculated according to Eq. 5 for instrument configurations *a* (original) and *b* (switched).

By dividing Eq. 7 by Eq. 8 and solving the detection efficiency η_{CPC},

$$\eta_{CPC} = \sqrt{\eta_a \cdot \eta_b \cdot \frac{\beta_b}{\beta_a}}. \tag{9}$$

Assuming that the bias remains constant during the measurements, β_a and β_b cancel each other and Eq. 9 reduces to

$$\eta_{CPC} = \sqrt{\eta_a \cdot \eta_b}. \tag{10}$$

The bias can then be calculated as

$$\beta = \sqrt{\eta_a / \eta_b}. \tag{11}$$

The bias may not remain constant throughout the experiments, though. That is, the ratio β_b / β_a in Eq. 9 may deviate from unity, such as

$$\beta_b / \beta_a = 1 + \delta, \tag{12}$$

where δ is the deviation from unity. The magnitude of δ is evaluated as the standard deviation of β obtained from the measurements at different particle sizes. The latter is considered to be equal to the standard uncertainty of β_b / β_a.

The standard uncertainty of the detection efficiency can be derived using the law of propagation of uncertainty as

$$u^2\left(\eta_{CPC}\right)=\frac{1}{4}\eta_{CPC}^2\cdot\left(\frac{u^2\left(\eta_a\right)}{\eta_a^2}+\frac{u^2\left(\eta_b\right)}{\eta_b^2}+u^2\left(\frac{\beta_b}{\beta_a}\right)\right). \tag{13}$$

According to Eq. 5, the standard uncertainty of the average detection efficiency in the configuration *a* (similarly for *b*) can be derived as

$$u^2\left(\eta_{\mathrm{a}}\right)=\eta_a^2\cdot\left(\frac{u^2\left(C_{CPC}\right)}{C_{CPC}^2}+\frac{u^2\left(C_{FCAE}\right)}{C_{FCAE}^2}\right). \tag{14}$$

For the CPC, the uncertainty can be estimated from the spread of the concentration values of ten repetitions (type A analysis):

$$u\left(C_{CPC}\right)=\frac{s\left(C_{CPC}\right)}{\sqrt{10}}, \tag{15}$$

which is the experimental standard deviation of the mean concentration. For the FCAE, the standard uncertainty of the FCAE number concentration (Eq. 1) can be expressed as

$$u^2\left(C_{FCAE}\right)=C_{FCAE}^2\left(\frac{u^2\left(\Delta I\right)}{\Delta I^2}+\frac{u^2\left(Q\right)}{Q^2}+\frac{u^2\left(\gamma\right)}{\gamma^2}+\frac{u^2\left(\eta_{\mathrm{FCAE}}\right)}{\eta_{FCAE}^2}+\frac{u^2\left(n\right)}{n^2}\right). \tag{16}$$

With the SCAR, the standard uncertainties for Q and γ are defined based on the calibration certificates of the applied instruments. The standard uncertainties for η_{FCAE} and n were already presented in Section 4.5. The offset corrected current is calculated as

$$\Delta I=I_{particle}-\frac{I_{offset-}+I_{offset+}}{2}-\delta\Delta I_i,\qquad (i=a,b). \tag{17}$$

Eq. 17 is almost identical with Eq. 2 in Section 3.1, except for the last term, which is an experimentally defined configuration dependent correction. This correction is needed only for the measurements performed using the setup I in Fig. 17. As noted in Paper IV, the toggling of the dilution flow rate (particles/no particles) causes a small pressure change in the FCAE (~0.1 mbar pressure change), which causes a momentary shift in the offset current. With the setup II, no correction is needed, and the standard uncertainty for the ΔI is calculated in the same fashion than the uncertainty of the CPC number concentration (Eq. 15). For both configurations (*a* and *b*), the corrections were determined experimentally in Paper IV. This was conducted by repeating the 21 min measurement routine 10 times using the same settings (e.g. temperatures) as in the actual measurements but without particles in the flow. The correction was then calculated as the average value of the ten repetitions. For the corrections, both the variation in the particle current during one measurement routine (duration 21 min) and the variation in the average value of ten 21 min repetitions were taken into account in the uncertainty evaluation. The average values for the corrections and the related standard uncertainties for configurations *a* and *b* are (1.0256 ± 0.3454) fA and (0.6889 ± 0.1407) fA, respectively. The standard uncertainty in the cases in which the correction is applied is calculated according to Eq. 18.

$$u^2\left(\Delta I\right)=s^2\left(\overline{\Delta I}\right)+u^2\left(\delta\Delta I_i\right)=\frac{s^2\left(\Delta I\right)}{10}+u^2\left(\delta\Delta I_i\right),\qquad (i=a,b). \tag{18}$$

The above uncertainty evaluation will have an important role in the next section, in which the overall performance of the SCAR in CPC calibrations, with respect to two other standards, will be presented based on the experiments conducted in Paper IV.

5.3. Overall performance

Probably the most reliable way to evaluate the overall performance of the SCAR, or any other NCS, is to compare it with other standards. During the work presented in Paper IV, the SCAR was transported to AIST (Japan) and a comparison between the SCAR and two other NCSs was conducted. The other number concentration standards were the FCAE based primary NCS of AIST (Sakurai and Ehara, 2011; Section 3.2) and the Inkjet Aerosol Generator of AIST (IAG; Iida et al., 2010). The comparison was performed by calibrating the same individual CPC with each of the three standards. All of the measurements were conducted in the same laboratory in order to guarantee the best achievable circumstances for detecting true differences between the standards. In total, the calibration results covered the particle size range from 10 nm up to 10 μm. The equivalence of the standards and the uncertainties associated with the calibration results were compared by studying the calibration results in the overlapping size ranges.

In the experiments, the calibrated instrument was a CPC 3772 (TSI Inc.), which has 1 L min^{-1} nominal flow rate (no sheath flow is used) and is capable of measuring concentrations up to 10^4 particles cm^{-3}. Particle size ranges and particle materials applied in the CPC calibration are summarized in Table 3.

Table 3. Particle size ranges and corresponding particle materials applied in the CPC calibration.

Calibration standard	sucrose	DOS	NaCl	PSL	water residue
Primary NCS of AIST	10 nm	12–66 nm	12–25 nm	50–300 nm	
SCAR		31 nm–1 μm	12 nm		
IAG of AIST			430 nm–11 μm		210 nm

With the primary NCS of AIST, most of the measurements were performed at three different concentrations: 3200, 5600 and 10000 particles cm^{-3}. With the SCAR, the measurements were conducted using an average concentration of 7850 particles cm^{-3}, which was selected in order to obtain a high signal-to-noise ratio for the FCAE. With the SCAR and the primary NCS of AIST, measurements were performed by using the measurement routine described in Section 5.1 and the results were calculated as described in Section 5.2. Thanks to the similar routines and types of the standards, it was possible to compare the individual uncertainty components contributing to the overall uncertainty of the detection efficiency between the two standards. In the IAG, a single nozzle from a printer head is used to generate monodisperse droplets from a solution consisting of NaCl and ultrapure water at a desired generation rate. After droplet evaporation, particles consisting of either NaCl or water residue are used for calibration purposes simply by attaching the IAG to the CPC inlet. In Paper IV, the IAG measurements were performed using 6 particles cm^{-3} number concentration. A more detailed description about the experiments at AIST can be found from Paper IV.

As a result of the experiments, a set of CPC calibrations was obtained for the particle size range from 10 nm to 11 µm, which practically covered the whole measurement range of the instrument. Fig. 18 shows all the results from the CPC 3772 calibration performed with the IAG and the SCAR. For the primary NCS of AIST, a calibration set obtained using 3200 particles cm^{-3} number concentration is shown.

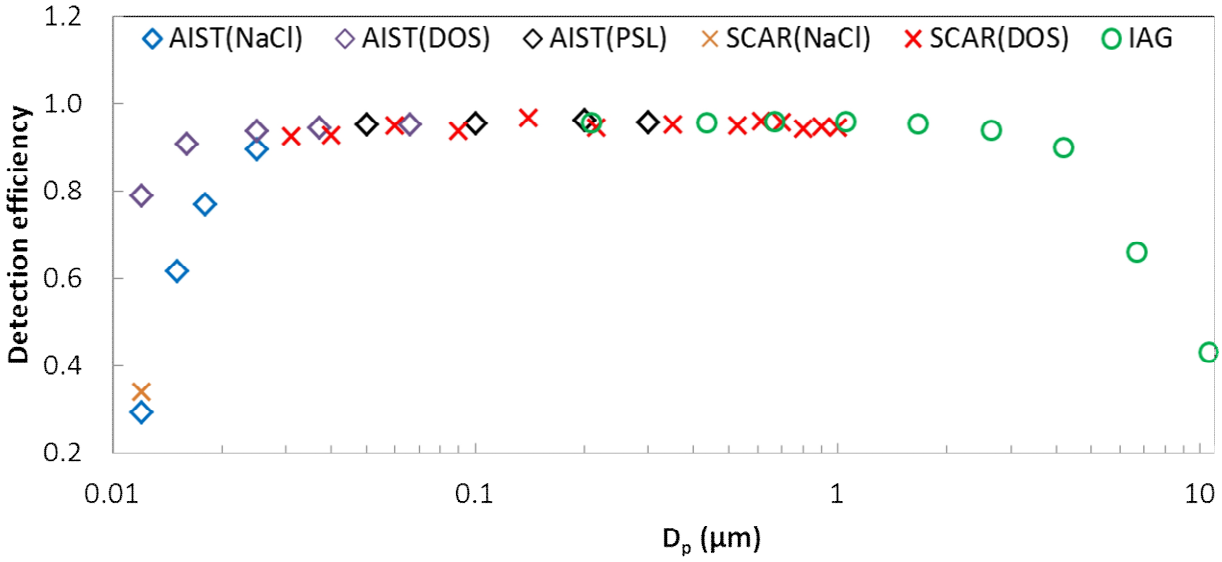

Figure 18. Calibration results for the same CPC 3772 (TSI Inc.) obtained using three different number concentration standards. Results with similar symbols are obtained with the same standard (Modified from Paper IV).

Regarding the comparison between the three NCSs, an adequate overlap in the size axis was achieved between the SCAR and the two other NCSs. Further, for the first time, the data in Fig. 18 provided an answer to an important question: how do condensation particle counters behave in their whole operating size range. In the lower size end, the results obtained with the primary NCS of AIST quite nicely demonstrate the dependence of the lower detection limit on particle material (e.g. Wang et al., 2010). Also, the plateau efficiency of a CPC is not always one (0.96 for this unit), and CPCs have a cut-off size also in the upper size end (9.3 µm for this unit). The results imply that this particular CPC could even be used for measuring the total number concentration for particles below 2.5 µm thus complementing the PM 2.5 filter-based mass measurement. This creates a new option for environmental monitoring.

In order to compare the three standards reliably, a particle size range in which the detection efficiency is practically unaffected by particle size and material was selected for further analysis from the data points presented in Fig. 18. Based on this criterion, the NaCl data was omitted from the AIST primary NCS and the SCAR. The rest of the results from 25 nm up to 1 µm were accepted. The selected results are shown in Fig. 19 together with the expanded uncertainties ($k = 2$, standard uncertainty multiplied by a factor of two).

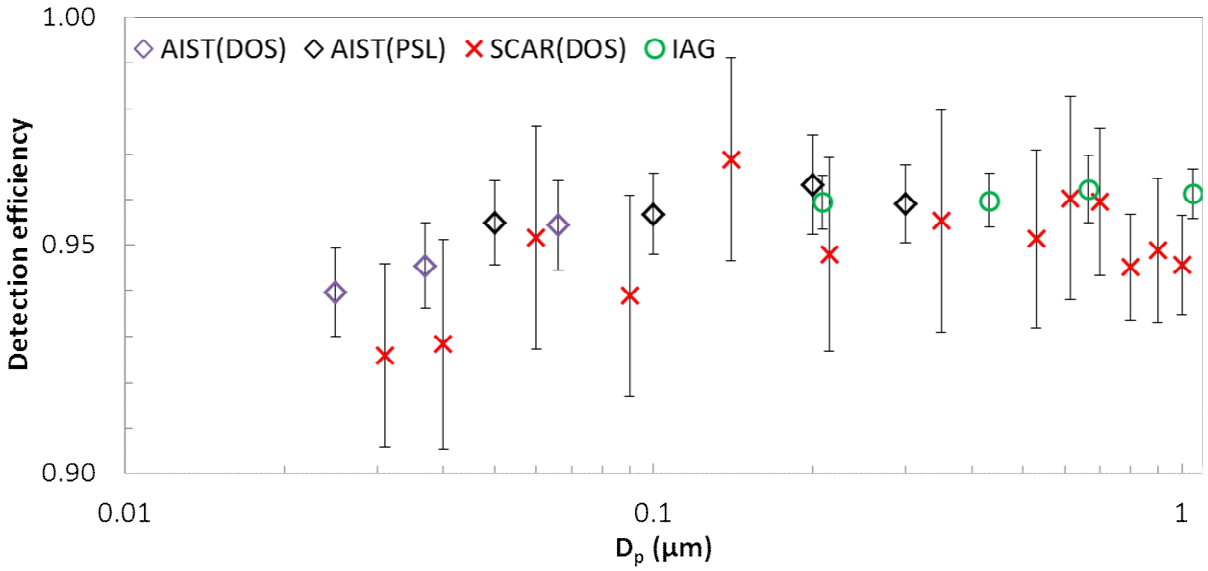

Figure 19. Close view of the calibration results obtained with the three different number concentration standards together with the related expanded uncertainties ($k = 2$) (Modified from Paper IV).

By looking at the results obtained for individual particle sizes in Fig. 19, it can be seen that the three standards agree within the uncertainty limits at all particle sizes. This is also true for the average detection efficiency values that were calculated for the three standards from the results in Fig. 19. This indicates that no separable systematic difference exist between the three standards. For all of the standards, this is a highly important result as it proves that the evaluation of the detection efficiency and its uncertainty has been performed correctly. The comparison conducted in Paper IV is very important since it was the first comparison that has been conducted by using primary number concentration standards of different countries and, in fact, the second comparison that has ever been conducted on a metrological level. In the first comparison, which was performed within the EURAMET Project 1027 (Schlatter, 2009), secondary standards (e.g. CPCs) from different countries were compared and found to agree within 5 % ($k = 2$). In Paper IV, the standards were found to agree within 0.5 % ($k = 2$), which is a major improvement in the field and can be seen as a pioneering act towards internationally coherent primary NCSs.

In the calibration measurements conducted in Paper IV, the relative expanded uncertainty values of the detection efficiency were between 1.1 and 2.6 % for the SCAR. These uncertainty values can be used as an indicator of the overall performance of the SCAR in calibration measurements. For the primary NCS of AIST, the corresponding values were between 0.8 and 1.1 %, and for the IAG, the respective values (sub-micrometer particles) were between 0.6 and 0.8 %. In order to discover what is causing the larger uncertainties with the SCAR compared to the AIST primary NCS, individual uncertainty components were compared between the two standards. Following the presentation in Section 5.2, Table 4 shows how the overall uncertainty for the detection efficiency is formed from the individual uncertainty components of the two standards.

Table 4. Typical values of the component uncertainties contributing to the overall standard uncertainty of the CPC detection efficiency calculated from the data in Fig. 19. The results apply to the following conditions: FCAE flow rate, 1 L min^{-1}; number concentration, 8500 and 3200 particles cm^{-3} for the SCAR and the primary NCS of AIST, respectively (Paper IV).

	SCAR		AIST
FCAE number concentration (Eq. 16)	Setup I	Setup II	
$\sqrt{\frac{u^2(Q)}{Q^2}+\frac{u^2(\gamma)}{\gamma^2}+\frac{u^2(\eta_{\mathrm{FCAE}})}{\eta_{FCAE}^2}+\frac{u^2(n)}{n^2}}$	0.004 64	0.004 64	0.003 94
$u(\Delta I)/\Delta I$	0.011 8	0.008 39	0.003 66
$u(C_{FCAE})/C_{FCAE}$	0.012 7	0.009 58	0.005 38
CPC number concentration			
$u(C_{CPC})/C_{CPC}$	0.004 84	0.001 79	0.001 71
Detection efficiency (conf. *a* or *b*) (Eq. 14)			
$u(\eta_{\mathrm{a\ or\ b}})/\eta_{\mathrm{a\ or\ b}}$	0.013 6	0.009 74	0.005 64
Bias between sampling ports			
$u(\beta_b/\beta_a)$	0.006 89	0.003 86	0.000 44
Overall detection efficiency (Eq. 13)			
$u(\eta_{\mathrm{CPC}})/\eta_{\mathrm{CPC}}$	0.010 2	0.007 15	0.004 00

The first uncertainty component from the top (the first row) in Table 4 includes all the uncertainty components related to the FCAE number concentration measurement except the uncertainty of the electric current measurement. Thus, the first row in Table 4 presents the minimum achievable uncertainty of the FCAE number concentration, which is about the same for the two standards. By looking at the whole table, it can be seen that the difference between the two standards is mainly caused by the uncertainty of the offset corrected current ($u(\Delta I)/\Delta I$) and by the uncertainty of the bias between the sampling ports ($u(\beta_b/\beta_a)$). The former is not related to the performance of the Faraday cup itself. Instead, it was found to be related to how the electrometer is configured to measure electric current. With the SCAR, one value per second was read and saved from the electrometer. Owing to software issues that have been solved by now, only a 20 ms integration time was used for the electrometer. This means that only 2 % of the theoretically possible measurement time was actually used. With the primary NCS of AIST, different settings were used for the electrometer and, as a consequence, the corresponding value was 83 %. After these measurements, completely new software has been developed for the electrometer of the SCAR. With the new software, more than 95 % of the theoretically possible measurement time is used which will reduce the uncertainty of the offset corrected current. The difference between the uncertainties of the bias between the sampling ports was recognized to be related to one important difference between the two calibration setups. In the primary NCS of AIST, a mixer was used

before the flow splitter in order to guarantee equal concentration inputs for the CPC and the FCAE. With the SCAR, no mixer was used in the setup I, which explains the large uncertainty value in Table 4. With the setup II, a mixer was used, but it was not connected to an optimal position (i.e. just before the flow splitter). Even so, using the mixer resulted in much better performance. During the later development of the SCAR, a mixer was added just before the flow splitter to both setups (I and II). With the improved measurement setup, the values for the concentration bias are typically smaller than 0.5 % (values as large as 5 % were reported in Paper IV). The improved setup is expected to reduce the uncertainty of the bias closer to the values that are typical for the AIST primary NCS. Equipped with the new electrometer software and with the flow mixer, the overall uncertainty of the results in future calibrations can be expected to reduce.

5.4. Future directions

The future of the SCAR is, in a good way, a mystery. The successful development of the instrument in the past and also some of its unique properties allows the development of the SCAR to various directions in the near future. The three most probable directions are developing the SCAR on a metrological, scientific or commercial level, which can all co-exist at the same time. On the metrological level, the main question is whether or not Finland should have its own primary standard laboratory for aerosol number concentration or for aerosol particles in general, and whether the primary standard should be established based on the SCAR. Although this issue has been discussed, so far no decisions have been made. Due to the newest European regulations concerning vehicle Particulate Matter emission (European Commission, 2008) and due to a number based emission limit set by the said regulations, the market for a certain type of CPCs is growing steadily. These CPCs are subjected to annual calibrations which increases the call for calibration services. This is one of the reasons why NMIs throughout Europe are starting to provide calibration services for CPCs. At this point, I am confident that the SCAR will have an important role in the aerosol particle metrology in the future.

The second direction, namely the scientific development, is an ongoing process at the Aerosol Physics Laboratory of Tampere University of Technology. One important goal of this work is to be able to generate solid, singly charged particles in a wide size range. The ability to produce calibration aerosols also from solid particles would increase the variety of applications to which the SCAR can be used. Another goal is to try to optimize the characteristics of the output size distribution. In practice, this means narrower size distributions and wider size and concentration ranges. To this end, some preliminary modeling work has been conducted using numerical simulations. In addition to the ongoing development, the SCAR should be applied to all kinds of measurements such as APS calibrations in the lower size end of its measuring range, impactor calibrations and characterizations of various chargers, to mention a few.

For the development of the SCAR on the commercial level, at least two alternatives exist. The first alternative is to license the SCAR to some of the existing companies. The second alternative is to found an enterprise partly based on the SCAR which has gained more and more interest over time. This enterprise could concentrate on calibrating the calibrators which are used to calibrate masses of instruments. Another option for the enterprise is to develop a simplified, low-cost version of the SCAR. This instrument could be designed to have as stable and repeatable output as the actual SCAR has but without any guarantee of singly charged particles.

6. Number concentration standards today

Within the last couple of years, aerosol particle metrology has developed substantially. New calibration laboratories have been founded and the capabilities of the existing ones have been extended. Some of the developments were already discussed in Section 3.2 in which the problem of multiple charging was presented. For many reasons, it would be interesting to know the current status of the existing and upcoming calibration services available for instruments that measure the number concentration of particles. Unfortunately, this kind of information is not found from the internet. Therefore, the author decided to approach the potential service providers directly by sending a simple table questionnaire. The main objective was to first collect the information into one place and then to share the information among the recipients thus increasing the common knowledge about existing services. The questionnaire was sent as an e-mail to several NMIs worldwide and also to other research laboratories. All of the recipients were known to deal with aerosols and they were requested to forward the e-mail to any other recipients that might contribute to this survey.

In the questionnaire, the quantities of particular interest were particle size ranges, respective concentration ranges, calibration particle materials and whether the standard was based on an FCAE or not. The total number of the recipients in the original survey, including TUT, was ten from whom the author received seven answers before the predetermined deadline. All of the results were then combined into a single table which was shared among the recipients and is shown in the following page (Table 5). Even though having the data from only seven different institutions may seem like a small fraction of the existing ones, it may, in fact, be the actual number of the institutes that currently have a genuinely traceable NCS.

The data in Table 5 shows that most of the standards are FCAE based with two exceptions, which are most likely designed for calibrating OPCs that are used in the clean rooms of production facilities at low concentration levels. Note that none of the standards is currently providing services for particles below 10 nm in diameter. This is a clear shortcoming. Practically all the existing FCAE based standards provide calibration services up to 100 nm. Two of them can reach 200 nm and only one, presented by Owen et al. 2012, can reach 400 nm. Thus, at the moment the SCAR is the only NCS that could provide calibrations up to 1 µm at number concentrations relevant for CPCs. Thanks to recent developments, the overall coverage of the standards is actually quite good. Probably the biggest issue is that some sizes and concentrations are available only from one place which may be located on the other side of the world with respect to the place were calibrations are needed. In order to solve this issue, the following steps should be taken. Firstly, the coherence of the existing primary NCSs should be verified. After the verification, these NCSs could be used for creating a network of secondary standards (e.g. CPCs) outside the NMIs. The secondary standards could then be made easily accessible to the end users. The mentioned procedure is currently conducted in a joint research project of the European Metrology Research Program called: Emerging requirements for measuring pollutants from automotive exhaust emissions. The Aerosol Physics Laboratory of TUT is included in this project.

Table 5. Worldwide coverage of the existing and upcoming calibration services for instruments that measure the number concentration of particles. The standard developed in this thesis is included and named as *Tampere University of Technology (FI), with Mikes*.

U.S. Army Primary Standards Laboratory (US)			**National Particle Laboratory (UK)**	
	range 1		range 1	
Size range (µm):	0.02-0.4		0.025-0.1	
Concentration (#/cm^3):	1-1e4		1e3-2e5	
FCAE based (Y/N):	Y		Y	
Particle material:	Emery oil		CAST-Soot	
Overall status:	operational		operational	
Physikalisch-Technische Bundesanstalt (DE)				
	range 1	range 2	range 3	
Size (µm):	0.01-0.1	0.005-0.05	0.005-0.05	
Concentration (#/cm^3):	1e3-1e5	1e3-1e4	1e3-1e4	
FCAE based (Y/N):	Y	Y	Y	
Particle material:	CAST-Soot, Propane	Ag	NaCl	
Overall status:	to be launched in June 2014			
National Institute of Advanced Industrial Science and Technology (JP)				
	range 1	range 2	range 3	
Size range (µm):	0.01-0.2	0.01-0.2	0.5-10	
Concentration (#/cm^3):	1e3-1e4	1-1e3	1-10	
FCAE based (Y/N):	Y	Y	N, IAG**	
Particle material:	PAO, PSL, Sucrose	PAO, PSL, Sucrose	NaCl, ionic liquids	
Overall status:	Operational	to be launched by 2013	to be launched by 2014	
Federal Office of Metrology METAS (CH)				
	range 1	range 2	range 3	range 4
Size range (µm):	0.02-0.2	0.02-0.08	0.02-0.05	0.1-5
Concentration (#/cm^3):	0-1e5	0-1e5	0-1e4	0-10
FCAE based (Y/N):	*	*	*	N
Particle material:	CAST-Soot	Ag	Au	PSL, LAPAZ***
Overall status:	Operational			
Tampere University of Technology (FI), with Mikes				
	range 1	range 2	range 3	
Size range (µm):	0.01-0.03	0.03-0.5	0.5-1.0	
Concentration (#/cm^3):	1e3-6e4	1e3-6e4	1e3-1e4	
FCAE based (Y/N):	Y	Y	Y	
Particle material:	NaCl	DOS	DOS	
Overall status:	no official services yet			
National Institute of Standards and Technology (US)				
services not available at the moment				

*The Swiss National Standard is based on the equivalence of the FCAE, CPC and OPC.

** Inkjet Aerosol Generator

*** Schlatter (2004)

7. Summary and conclusions

The main objective in this thesis was to develop new aerosol instrumentation both for measurement and calibration purposes. On the measurement side, the nanoparticle resolution of the well-known ELPI (Dekati Ltd.) was improved. This was achieved by designing, manufacturing and implementing a new impactor stage with an experimentally verified cutpoint of 16.7 nm to the ELPI cascade impactor. The new stage divides the size range measured by the filter stage (7–30 nm) between the new stage and the filter stage. As a consequence, the nanoparticle resolution of the ELPI was improved. This resulted in better performance for example in engine emission measurements. The new stage is currently sold as a part of the new ELPI+ impactor, which is a completely renewed version of the original ELPI.

On the calibration side, a new primary Number Concentration Standard (NCS) was developed. From the development of the new standard, three phases can be identified: proof of concept, validation and intercomparison. In the first phase, a new instrument called the Singly Charged Aerosol Reference (SCAR) was designed, built and tested. This new device combines a novel principle for the generation of a singly charged calibration aerosol with traceable Faraday cup Aerosol Electrometer (FCAE) based number concentration measurements in order to realize a number concentration standard. In the first experiments, the SCAR was demonstrated to produce singly charged, fairly monodisperse calibration aerosols between 10 nm and 500 nm suitable for calibration purposes. In the second phase, the operation of the SCAR was thoroughly characterized in co-operation with MIKES–the Centre for Metrology and Accreditation (Finland) with the following results. The average charge of the particles equals to one elementary charge up to 500 nm in size with 0.16 % relative standard uncertainty. As a result of the validation, a true SI-traceability for the particle number concentration output of the SCAR was formed, and consequently a new primary NCS was established. In calibration measurements, the standard uncertainty for the output number concentration is typically around 1 % which is mainly caused by the uncertainties in the electric current and volumetric flow rate measurements of the FCAE.

As a final step in the SCAR's development towards becoming an internationally recognized primary NCS, a comparison between the SCAR and two other NCSs of the National Institute of Advanced Industrial Science and Technology (AIST) was conducted in Japan. The other standards were: the primary NCS of AIST and the Inkjet Aerosol Generator (IAG) of AIST. The comparison was performed by calibrating the same individual CPC with each standard. Overall, the calibration results covered the size range between 10 nm and 10 µm, which has never been accomplished before. In the experiments of this study, the operating particle size range of the SCAR was extended up to 1 µm. The results obtained with the three standards were found to agree at all overlapping particle sizes within the uncertainty limits. The determined relative expanded uncertainties (k = 2) for the detection efficiency were between 0.8 and 1.1 % for the primary NCS of AIST, between 0.6 and 0.8 % for the IAG of AIST and between 1.1 and 2.6 % for the SCAR. The overall agreement between the standards was found to be within 0.5 %. From the metrological point of view, the conducted comparison is very important because it is the first one that has ever been conducted using the primary number concentration standards of different countries. As a consequence of all three phases, a new primary NCS, which enables accurate calibrations of various instruments in the whole sub-micrometer range, has been established.

References

Agarwal, J.K. and Sem, G.J. (1980) Continuous flow, single-particle counting condensation nucleus counter. *J. Aerosol Sci*. **11**, 343-357.

Armendariz, A.J. and Leith, D. (2002) Concentration measurement and particle counting efficiency for the aerodynamic particle sizer 3320. *J. Aerosol Sci.* **33**, 133-148.

Banse, D.F., Esfeld, K., Hermann, M., Sierau, B., Wiedensohler, A. (2001) Particle counting efficiency of the TSI CPC 2762 for different operating parameters. *J. Aerosol Sci.* **32**, 157-161.

Baron, P. A. (1984) "Aerodynamic particle sizer calibration and use, aerosols: science, technology, and industrial applications of airborne particles," Proceedings of the First International Aerosol Conference, Publ by Elsevier, New York, NY, USA and Amsterdam, Neth, 215-216)

Barthazy, E., Stetzer, O., Derungs, C., Wahlen, S. and Lohmann, U. (2007) Characterization of a propane soot generator *Nucleation and atmospheric aerosols, 17th International Conference, Galway, Ireland*, ed C D O'Dowd and P E Wagner (Berlin: Springer), 834–839.

Bartz, H., Fissan, H. and Liu, B. Y. H. (1987) A New Generator for Ultrafine Aerosols Below 10 nm. *Aerosol Sci. Technol*. **6**,163 — 171.

Berglund, R. N. & Liu, B. Y. H. (1973) Generation of Monodisperse Aerosol Standards. *Environ. Sci. Tech.* **7**, 147-153.

Biskos, G., Reavell, K., & Collings, N. (2005) Description and theoretical analysis of a differential mobility spectrometer. *Aerosol Sci. Technol.*, ***39***, 527–541.

CAFE (Clean Air For Europe). (2001). The Clean Air for Europe Programme: Towards a Thematic Strategy for Air Quality. European Commission. Available online at http://eur-lex.europa.eu/LexUriServ.do?uri = CELEX:52001DC0245:EN:NOT

Chen, D.-R., Pui, D. Y.H., & Kaufman, S. L. (1995). Electrospraying of conducting liquids for monodisperse aerosol generation in the 4 nm–1.8 mm diameter range. *J. Aerosol Sci.* **26,** 963–977.

Ehara, K. and Sakurai, H. (2010) Metrology of airborne and liquid-borne nanoparticles: current status and future needs. *Metrologia* **47,** 83-90.

European Commission. (2008). Regulation No. 692. Implementing and Amending Regulation (EC) No. 715/2007 of the European Parliament and of the Council on Type-Approval of Motor Vehicles with Respect to Emissions from Light Passenger and Commercial Vehicles (Euro 5 and Euro 6) and on Access to Vehicle Repair and Maintenance Information. *Offic. J. Eur. Union*, L:199/1.

EUSAAR (European Supersites for Atmospheric Aerosol Research) webpage, www.eusaar.net, [14.6.2012]

Filippo, A. D., Maricq, M. M. (2008) Diesel Nucleation Mode Particles:Semivolatile or Solid? *Environ. Sci. Technol*., **42**, 7957 – 7962.

Fletcher, R.A., Mulholland, G.W., Winchester, M.R., King, R.L., and Klinedinst, D.B. (2009) Calibration of a Condensation Particle Counter Using a NIST Traceable Method. *Aerosol Sci. Technol.*, **43**, 425-441.

Fuchs, N. A. (1963) On the stationary charge distribution on aerosol particles in a bipolar ionic atmosphere. *Pure and Applied Geophysics* **56**, 185-193.

Gormley, P.G. and Kennedy, M. (1949) Diffusion from a stream flowing through a cylindrical tube. *Proc. R. Irish Acad. A.* **52**, 163-169.

Hermann, M., Wehner, B. Bischof, O., Han, H.-S., Krinke, T., Liu, W., Zerrath, A., and Wiedensohler, A. (2007) Particle counting efficiencies of new TSI condensation particle counters. *J. Aerosol Sci*. **38**, 674-682.

Hillamo, R.E. and Kauppinen, E.I. (1991) On the performance of the Berner type low pressure impactor. *Aerosol Sci. Technol.* **14**, 33-47.

Hinds, W.C. 1998. Aerosol Technology. Properties, Behavior, and Measurement of Airborne Particles. 2nd ed. New York, John Wiley & Sons inc. 483 p.

Hoppel, W.A. (1978) Determination of the aerosol size distribution from the mobility distribution of the charged fraction of aerosols. *J. Aerosol Sci.* **9**, 41-54.

Iida, K., Sakurai, H., Saito, K., Ehara, K. (2010) An Inkjet Aerosol Generator for Calibrating Particle Counters. *Abstract book of International Aerosol Conference 2010 Helsinki*, Poster Number P1E59, http://www.atm.helsinki.fi/IAC2010/abstracts/abstbook.html

IPCC (The Intergovernmental Panel on Climate Change). (2007). Intergovernmental Panel on Climate Change Fourth Assessment Report: Climate Change 2007 (AR4). The Physical Science Basis. Solomon, S., D. Qin, M. Manning, Z. Chen, M. Marquis, K. B. Averyt, M. Tignor, and H. L. Miller, eds. Cambridge University Press, Cambridge, UK, and New York.

ISO 14644-1. (1999). Cleanrooms and Associated Controlled Environments—Part 1: Classification of Air Cleanliness. International Organization for Standardization, Geneva, Switzerland.

Jing webpage, www.sootgenerator.com/midCAST_spec.htm, [20.2.2012]

Kauppinen, E.I., Hillamo, R.E. (1989) Modification of the University of Washington Mark-5 in-stack impactor. *J. Aerosol Sci.* **20**, 813-827.

Keskinen, J., Pietarinen, K. and Lehtimäki, M. (1992) Electrical Low Pressure Impactor. *J. Aerosol Sci.* **23**, 353-360.

Keskinen, J., Marjamäki, M., Virtanen, A., Mäkelä, T., Hillamo, R. (1999) Electrical Calibration Method for Cascade Impactors. *J Aerosol Sci*. **30**, 111-116.

Kittelson, D. (1998) Engines and Nanoparticles: A Review. *J. Aerosol Sci.* **29**, 575–588.

Knollenberg, R.G. and Luehr, R. (1976) Open cavity laser "active" scattering particle spectroscopy from 0.05 to 5 microns. In *Fine Particles- Aerosol Generation, Measurement, sampling, and Analysis*, Liu, B.Y.H., ed. Academic Press, London, 669-696.

Koch,W., Pohlmann,G., and Schwarz, K., (2008) A reference number concentration generator for ultrafine aerosols based on Brownian coagulation. *J. Aerosol Sci.* **39,** 150–155.

Kulmala, M., Riipinen, I., Sipilä, M., Manninen, H.E., Petäjä, T., Junninen, H., Dal Maso, M., Mordas, G., Mirme, A., Vana, M., Hirsikko, A., Laakso, L., Harrison, R.M., Hanson, I., Leung, C., Lehtinen, K.E.J., Kerminen, V.-M. (2007) Toward direct measurement of atmospheric nucleation. *Science*, **318** (5847), 89-92.

Liu, B.Y.H. and Lee, K.W. (1975). An Aerosol Generator of High Stability. *Am. Ind. Hyg. Assoc. J.* **36,** 861–865.

Liu, B.Y.H., Kim, C.S. (1977) On the counting efficiency of condensation nuclei counters. *Atmospheric Environment* **11**, 1097-1100.

Liu, B.Y.H., Pui, D.Y.H., Hogan, A.W., and Rich, T.A. (1975) Calibration of the Pollak Counter with Monodisperse Aerosols. *J. Appl. Met*. **14**, 46-51.

Marjamäki, M., Ntziachristos, L., Virtanen, A., Ristimäki, J., Keskinen, J., Moisio, M., Palonen, M. and Lappi, M. (2002). Electrical Filter Stage for the ELPI. *SAE Technical Paper Series* 2002-01-0055.

Marshall, I. (2007) Particle Number Counter Calibration Procedures. AEA Energy & Environment, http://www.unece.org/trans/doc/2008/wp29grpe/PMP-PNC-Calibration Procedure. pdfS.

Mirme, A. and Tamm, E. (2002). Electrical Classification in Wide Diameter Range, In Abstracts of Sixth International Aerosol Conference, 1073–1074, Taipei, Taiwan.

Mordas, G., Manninen, H. E., Petäjä, T., Aalto, P. P., Hämeri, K. and Kulmala, M. (2008) On Operation of the Ultra-Fine Water-Based CPC TSI 3786 and Comparison with Other TSI Models (TSI 3776, TSI 3772, TSI 3025, TSI 3010, TSI 3007). *Aerosol Sci. Technol.* **42**, 152-158.

NSF. (June 27–28, 2003). Workshop Report on "Emerging Issues in Nanoparticle Aerosol Science and Technology (NAST)". University of California, Los Angeles.

Okuyama, K., Shimada, M., Choi, M., Han, B. United States patent application 20050180543. Aerosol particle classification apparatus 2005.

Owen, M., Mulholland, G. and Guthrie, W. (2012) Condensation particle counter proportionality calibration from 1 particle·cm^{-3} to 10^{4} particles·cm^{-3}. *Aerosol Sci. Technol.*, **46**, 444–450.

Rader, D. J., McMurry, P. H. & Smith, S. (1987) Evaporation Rates of Monodisperse Organic Aerosols in the 0.02- to 0.2-µm-Diameter Range. *Aerosol Sci. Technol.* **6**, 247-260.

Ristovski, Z. D., Morawska, L. and Bofinger, N. D. (1998) Investigation of a modified Sinclair-la mer aerosol generator in the submicrometer range. *J. Aerosol Sci*. **29**, 799–809.

Rönkkö, T., Virtanen, A., Kannosto, J., Keskinen, J., Lappi, M. and Pirjola, L. (2007) Nucleation Mode Particles with a Nonvolatile Core in the Exhaust of a Heavy Duty Diesel Vehicle. *Environ. Sci. Technol.* **41**, 6384–6389.

Sakurai, H. and Ehara, K. (2010) A method for traceable calibration of condensation particle counters at low concentrations. In *Abstracts of the AAAR 29th annual conference,* Oregon, USA, Poster Number 2F.20.

Sakurai, H. and Ehara, K. (2011) Evaluation of uncertainties in femtoampere current measurement for the number concentration standard of aerosol nanoparticles. *Meas. Sci. Technol.* **22** 024009

Schlatter, J. (2004) LAPAZ—A laser particle counter as a primary number concentration standard. In *Abstracts of the European aerosol conference*, Budapest, Hungary, September 2004, **6**, 901–902.

Schlatter, J. (2009) *Final Report of EURAMET Project 1027* (www.euramet.org)

Schneider, J., Hock, N., Weimer, S., Borrmann, S., Kirchner, U., Vogt R., and Scheer, V. (2005) Nucleation particles in diesel exhaust: Composition inferred from in situ mass spectrometric analysis. *Environ. Sci. Technol*.,**39**, 6153–6161.

Sem, G.J. (2002) Design and performance characteristics of three continuous-flow condensation particle counters: a summary. *Atmospheric Research* **62**, 267-294.

Shimada, M., Han, B., Okuyama, K. and Otani, Y. (2002) Bipolar charging of aerosol nanoparticles by a soft x-ray photoionizer. *J. Chem. Eng. Japan* **35**, 786-793.

Sillanpää, S., Niederhauser, B., and Heinonen, M. (2006) Comparison of primary low gas flow standards between MIKES and METAS. *Measurement* **39**, 26-33.

Takegawa, N. and Sakurai, H. (2011) Laboratory evaluation of a TSI condensation particle counter (model 3771) under airborne measurement conditions. *Aerosol Sci. Technol.* **45**, 272 - 283.

Uin, J., Tamm, E. and Mirme, A. (2009) Electrically produced standard aerosols in wide size range. *Aerosol Sci. Technol.* **43**, 847 – 853.

Volckens, J. And Peters, T.M. (2005) Counting and particle transmission efficiency of the aerodynamic particle sizer. *J. Aerosol Sci.* **26**, 1400-1408.

Wang, H.-C., John, W. (1988) Characteristics of the Berner impactor for sampling inorganic ions. *Aerosol Sci. Technol.* **8.** 157-172.

Wang, S. C., Flagan, R. C. (1990) Scanning electrical mobility spectrometer. *Aerosol Sci. Technol.* **13,** 230-240.

Wang, X., Caldow, R., Sem, G. J., Hama, N. and Sakurai, H. (2010) Evaluation of a condensation particle counter for vehicle emission measurement: Experimental procedure and effects of calibration aerosol material. *J. Aerosol Sci.* **41,** 306-318.

WCCAP (World Calibration Centre for Aerosol Particles) webpage, http://gaw.tropos.de/WCCAP/index.html, [14.6.2012]

Wiedensohler, A. (1988) An approximation of the bipolar charge distribution for particles in the submicron size range. *J. Aerosol Sci*. **19**, 387-389.

Wiedensohler, A., Birmili, W., Nowak, A., Sonntag, A., Weinhold, K., Merkel, M., Wehner, B., Tuch, T., Pfeifer, S., Fiebig, M., Fjäraa, A. M., Asmi, E., Sellegri, K., Depuy, R., Venzac, H., Villani, P., Laj, P., Aalto, P., Ogren, J. A., Swietlicki, E., Williams, P., Roldin, P., Quincey, P., Hüglin, C., Fierz-Schmidhauser, R., Gysel, M., Weingartner, E., Riccobono, F., Santos, S., Grüning, C., Faloon, K., Beddows, D., Harrison, R., Monahan, C., Jennings, S. G., O'Dowd, C. D., Marinoni, A., Horn, H.-G., Keck, L., Jiang, J., Scheckman, J., McMurry, P. H., Deng, Z., Zhao, C. S., Moerman, M., Henzing, B., de Leeuw, G., Löschau, G., and Bastian, S. (2012) Mobility particle size spectrometers: harmonization of technical standards and data structure to facilitate high quality long-term observations of atmospheric particle number size distributions. *Atmos. Meas. Tech*. **5**, 657-685.

Wright, J., Mattingly, G., Nakao, S., Yokoi, Y., and Takamoto, M. (1998) International Comparison of a NIST Primary Standard with an NRLM Transfer Standard for Smalle Mass Flow Rates of Nitrogen Gas. *Metrologia* **35**, 211-221.

Tampereen teknillinen yliopisto
PL 527
33101 Tampere

Tampere University of Technology
P.O.B. 527
FI-33101 Tampere, Finland

ISBN 978-952-15-2925-2
ISSN 1459-2045